

AD \_\_\_\_\_

Award Number: W81XWH-08-1-0509

**TITLE:** The Role of BRCA1 Domains and Motifs in Tumor Suppression

**PRINCIPAL INVESTIGATOR:** Aneliya Velkova

**CONTRACTING ORGANIZATION:** H. Lee Moffitt Cancer Center  
Tampa, FL 33612

**REPORT DATE:** August 2010

**TYPE OF REPORT:** Annual Summary

**PREPARED FOR:** U.S. Army Medical Research and Materiel Command  
Fort Detrick, Maryland 21702-5012

**DISTRIBUTION STATEMENT:** Approved for Public Release;  
Distribution Unlimited

The views, opinions and/or findings contained in this report are those of the author(s) and should not be construed as an official Department of the Army position, policy or decision unless so designated by other documentation.

# REPORT DOCUMENTATION PAGE

Form Approved  
OMB No. 0704-0188

Public reporting burden for this collection of information is estimated to average 1 hour per response, including the time for reviewing instructions, searching existing data sources, gathering and maintaining the data needed, and completing and reviewing this collection of information. Send comments regarding this burden estimate or any other aspect of this collection of information, including suggestions for reducing this burden to Department of Defense, Washington Headquarters Services, Directorate for Information Operations and Reports (0704-0188), 1215 Jefferson Davis Highway, Suite 1204, Arlington, VA 22202-4302. Respondents should be aware that notwithstanding any other provision of law, no person shall be subject to any penalty for failing to comply with a collection of information if it does not display a currently valid OMB control number. PLEASE DO NOT RETURN YOUR FORM TO THE ABOVE ADDRESS.

1. REPORT DATE (DD-MM-YYYY) 08/31/10			2. REPORT TYPE Annual summary		3. DATES COVERED 1 Aug 2009-31 July 2010	
4. TITLE AND SUBTITLE The Role of BRCA1 Domains and Motifs in Tumor Suppression					5a. CONTRACT NUMBER	
					5b. GRANT NUMBER	W81XWH-08-1-0509
					5c. PROGRAM ELEMENT NUMBER	
6. AUTHOR(S) Aneliya Velkova  Email: aneliya.velkova@moffitt.org					5d. PROJECT NUMBER	
					5e. TASK NUMBER	
					5f. WORK UNIT NUMBER	
7. PERFORMING ORGANIZATION NAME(S) AND ADDRESS(ES)  H. Lee Moffitt Cancer Center & Research Institute, Inc. 12902 Magnolia Drive Tampa Fl 33612					8. PERFORMING ORGANIZATION REPORT NUMBER	
9. SPONSORING / MONITORING AGENCY NAME(S) AND ADDRESS(ES) U.S. Army Medical Research and Materiel Command Fort Detrick, Maryland 21702-5012					10. SPONSOR/MONITOR'S ACRONYM(S)	
					11. SPONSOR/MONITOR'S REPORT NUMBER(S)	
12. DISTRIBUTION / AVAILABILITY STATEMENT  Approved for public release; distribution unlimited						
13. SUPPLEMENTARY NOTES						
14. ABSTRACT The purpose of this research is to classify <i>BRCA1</i> variants for which cancer association is not known (unclassified variants UCV). To approach this problem we hypothesized that poorly characterized but conserved domains in <i>BRCA1</i> directly participate in its tumor suppression function. To test this hypothesis we choose a global approach analyzing several <i>BRCA1</i> domains and point mutants in functions that have previously been attributed to <i>BRCA1</i> : long term survival after irradiation, early G2/M checkpoint, intra S phase checkpoint, and spindle assembly checkpoint. We successfully optimized conditions for expression of full-length <i>BRCA1</i> mutants in two different cell lines by electroporation and lipofectamine based transfection. We analyzed all the <i>BRCA1</i> mutants proposed in this application. Our analysis revealed that the coiled-coil domain of <i>BRCA1</i> is important for the intra-S-phase checkpoint function of <i>BRCA1</i> . We also begin to characterize two conserved motifs of <i>BRCA1</i> : Motif 6 (proposed in this application) and Motif 2 (as a new finding). This will have a significant impact not only to understand <i>BRCA1</i> role as a tumor suppressor in breast cancer but also to help patients that are carriers of <i>BRCA1</i> mutation to make informed clinical decisions.						
15. SUBJECT TERMS BRCA1, unclassified variants, genetic counseling, Breast cancer treatment						
16. SECURITY CLASSIFICATION OF:			17. LIMITATION OF ABSTRACT	18. NUMBER OF PAGES	19a. NAME OF RESPONSIBLE PERSON USAMRMC	
a. REPORT U	b. ABSTRACT U	c. THIS PAGE U	UU	23	19b. TELEPHONE NUMBER (include area code)	

## Table of Contents

	<u>Page</u>
<b>Introduction.....</b>	<b>1</b>
<b>Body.....</b>	<b>1-4</b>
<b>Key Research Accomplishments.....</b>	<b>5</b>
<b>Reportable Outcomes.....</b>	<b>4-5</b>
<b>Conclusion.....</b>	<b>5</b>
<b>Appendices.....</b>	<b>6-20</b>

## I. Introduction: Summary of project objectives and scope of research

Breast cancer is among the most frequent malignancies affecting women. Germline mutations in the breast and ovarian cancer predisposition gene 1 (*BRCA1*) are responsible for the majority of early-onset hereditary breast cancers arising in families with multiple cases. It is estimated that around 10% of all women undergoing testing and about 35-50% of women from minority populations receive non-informative results, due to the finding of a variant for which cancer association is not known. These are called unclassified variants (UCVs). Considering that there are over 1500 alleles of *BRCA1*, one of the most challenging tasks for genetic counseling is to distinguish which are benign and which are cancer predisposing. Previous research has indicated that the likelihood of a variant being deleterious is higher when the variant is located in a structurally and functionally defined protein domain. Thus, the identification of other functional domains is critical to classifying variants. To approach this problem we hypothesized that poorly characterized, conserved domains in the central region of *BRCA1* (called motif 6 and coiled-coil domain) directly participate in tumor suppression functions of *BRCA1*. This proposal aims to test our hypothesis and determine how specific domains and motifs of *BRCA1* act to promote tumor suppression. Importantly our research has much broader implications because gene products implicated in breast cancer seem to cluster around DNA damage response pathways. Thus, an understanding of the role of *BRCA1* will likely have an impact on other forms of breast cancer not attributable to germline mutations in *BRCA1*. Both radiation therapy and most of the drugs used for cancer treatment rely on introducing DNA damage in the cells. *BRCA1* is a main participant in the cellular response to DNA damage, which makes it a very important factor in modulating the patient's response to therapy.

## II. Key research accomplishments

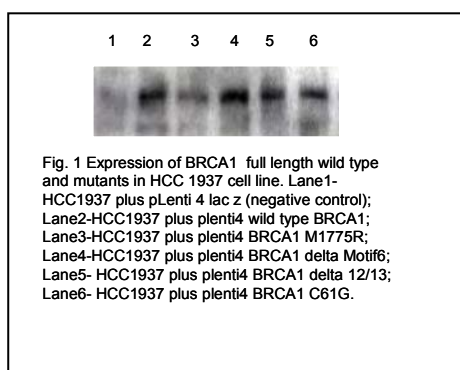
*We are on target to complete all tasks in the timeframe proposed.*

*Task 1. To determine the functional significance of two poorly characterized domains of *BRCA1* (Months 1-24):*

*1a. Generating *BRCA1* C61G in pLenti4 *BRCA1* full length. Task 1a is completed (see previous report)*

*1b. Generating *BRCA1*-null cell lines with reconstituted full-length *BRCA1*C61G. Fig.1 shows a typical experiment of ectopic expression of full-length *BRCA1* and mutants in HCC1937 cell line. Expression of *BRCA1* C61G mutant is shown in lane 6. Thus, task 1b is completed.*

*1c. Verifying the expression levels and subcellular localization of *BRCA1* wt and mutants (C61G, M1775R, delta motif 6 and delta exon 12/13) in SUM1315 tet repressor, SUM149 tet repressor and HCC1937 tet repressor cell lines. We verified the expression levels of full-length *BRCA1* and mutants in HCC1937 cell line (Fig.1).*



Unfortunately we could not test the proper nuclear localization of *BRCA1* mutants and the ability of *BRCA1* to form normal S-phase foci because the most appropriate antibody for these purposes, *BRCA1* Ab3 antibody (Calbiochem), was discontinued and currently it is not available commercially. We also tested two additional *BRCA1* antibodies but none of them worked properly for immunofluorescence. Thus, we propose to revise this task and analyze all *BRCA1* mutants using an alternative method of cellular fractionation (nuclear and cytoplasmic fractions), followed by western blot with *BRCA1* Ab1 antibody.

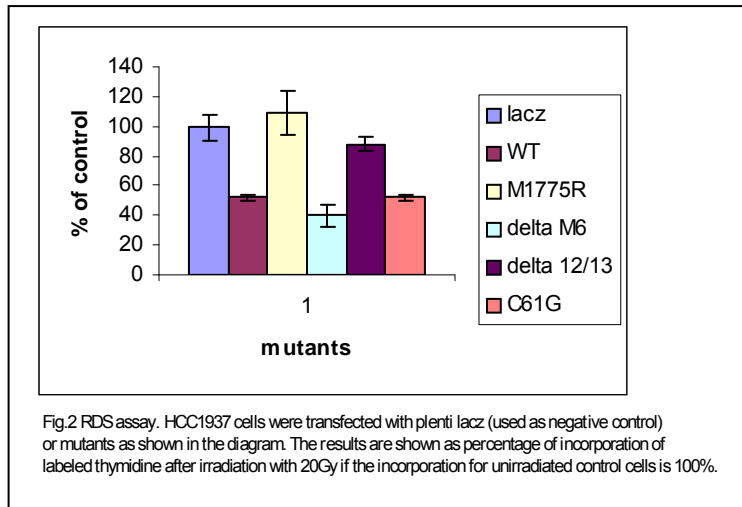
1d. *Colony forming assay after irradiation.* We performed colony forming assays with HCC1937 transfected with pLenti plasmids expressing either BRCA1 wild type or mutant constructs: M1775R, a mutant lacking Motif 6 (delta motif 6), a mutant lacking sequences in exons 12 and 13 that code for the coiled-coil domain (delta 12/13), and BRCA1 C61G mutant. We used HCC1937 cell line transfected with pLenti lacZ plasmid as a negative control. Our experiments indicate that HCC1937 expressing BRCA1 wild type and delta Motif 6, showed better survival after ionizing radiation than HCC1937 expressing lacZ, delta 12/13, C61G or M1775R mutants. This suggests that the RING, coiled-coil and BRCT domains are critical for survival after irradiation. Thus, task 1d is completed.

1e. *Early G2/M checkpoint assay.* We initially tested wt BRCA1 and mutants proposed in the application for early G2/M checkpoint. The results from several independent experiments with multiple samples revealed that this assay does not seem to be sensitive enough in our conditions. This may be due to several reasons:

- Transfection of HCC1937 cells (even with negative control plasmid pLenti lacZ) influences the percentage of cells in mitosis.
- The ectopic expression of the BRCA1 mutants is variable. In the G2/M assay we measure the changes in the G2/M phase of the cell cycle, which for HCC1937 cells represent ~2% of the total cell population. Transfection efficiency is well under 100% and this compounds the technical issue.
- SUM1315 and SUM 149 cell lines, which were our other options for BRCA1 negative cell lines, behaved as they have intact G2/M checkpoint in our analysis so we conclude that they do not constitute a viable alternative.

Thus, even though we tested all the BRCA1 mutants, proposed in the application we concluded that the early G2/M assay using ectopic transfection is not sensitive enough under these conditions to be used for functional analysis of unclassified variants of BRCA1. Thus, task 1e is completed.

1f. *RDS (radioresistant DNA synthesis) assay.* We performed RDS assay using HCC1937 cell line, transfected with all the mutants proposed in the application (Fig. 2). We used HCC1937 cell line transfected with pLenti lacZ plasmid as a negative control.



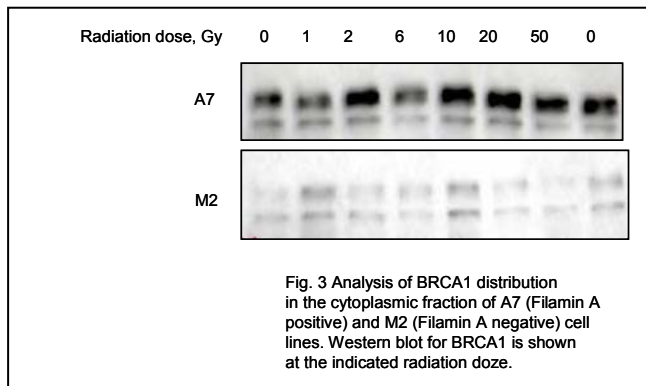
Our results (Fig.2) show that Motif 6 (delta M6) and RING domain (C61G) are not required for the intra-S-phase checkpoint function of BRCA1. On the other hand the coiled-coiled (delta 12/13) and BRCT (M1775R) domains are necessary for the intra-S-phase checkpoint. We conclude that the RDS assay can be used for testing the function of BRCA1 UCVs and plan to increase the number of variants that we will be testing for the future. We also plan to use this assay routinely in our laboratory to understand the mechanism by which BRCA1 controls the intra-S-phase checkpoint.

These results constitute the basis of a planned manuscript submission. Thus, task 1f is completed.

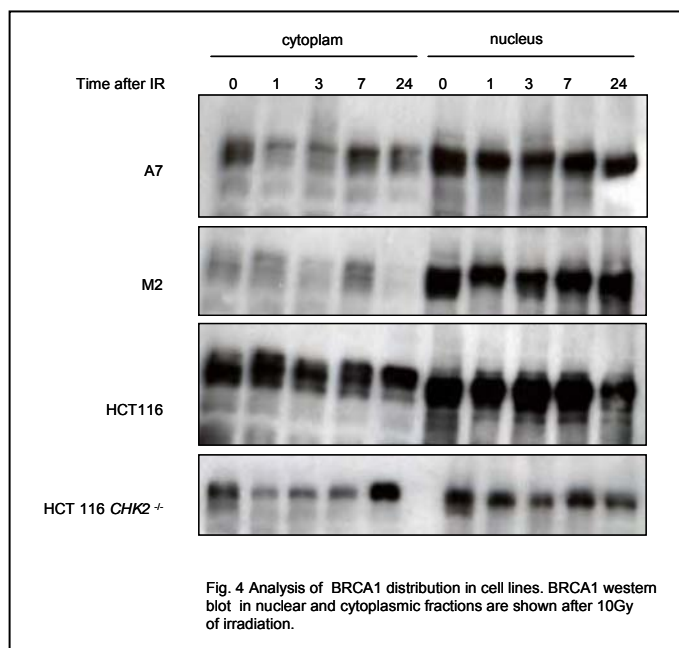
1g. *Assay for intact spindle assembly checkpoint.* We used HCC1937 cell line transfected with pLenti lacZ (as negative control) or with pLenti BRCA1 wild type (as positive control) and analyzed phosphohistone H3 positive cells after nocodazole treatment (spindle assembly checkpoint). There was no difference between the two samples (positive and negative control) in any of the time points examined i.e. the wild type BRCA1 could not reconstitute the spindle assembly checkpoint in HCC1937 cell line. Unfortunately, the function of BRCA1 in spindle assembly checkpoint has been extensively tested in mouse embryonic fibroblasts not in human breast cancer epithelial cell lines. We speculate that the

difference may be species specific. Thus, we conclude that the spindle assembly assay cannot discriminate different alleles of BRCA1. Thus, task 1g is completed.

**Task2.** To characterize the interaction between Filamin A and conserved motif 6 (months 18-36).



**2a. Performing dose response and time course analysis in M2, A7, HCT116, HCT116 *chk2*<sup>-/-</sup> cell lines.** We started by analyzing BRCA1 levels in the cytoplasmic fraction of A7 (Filamin A positive) and M2 (Filamin A negative cell line). At all time points tested M2 cell lines showed significantly lower levels of BRCA1 as expected (Fig. 3). We choose 10 Gy (maximum levels of BRCA1 in A7 cells) and performed detailed time course analysis (0-24h) of BRCA1 distribution in several cell lines (Fig.4).



Next, we analyzed the BRCA1-P-988 antibody. Unfortunately, these experiments revealed several shortcomings of this reagent. First, this phospho-specific antibody recognizes a band corresponding to BRCA1 in HCT116 *CHK2*<sup>-/-</sup> cell line. Phosphorylation of Ser-988 in BRCA1 is thought to be mediated by CHK2. Thus, this cell line should not present with this phospho epitope. Second, we used shRNAs against BRCA1 to make sure that the antibody indeed recognizes the correct (BRCA1) epitope. There was no difference between scrambled shRNA and shRNA for BRCA1 when using phospho-BRCA1-988 for western blot, although the endogenous BRCA1 was effectively silenced. Thus we conclude that this reagent (BRCA1-P-988 antibody) cannot be used with confidence. At this time there is no other alternative vendor or antibody. Thus, task 2a is completed.

**2b. Confirming dose response and time course analysis in MCF7 breast cancer cell line.** This task will be performed within next year grant period according to the original plan.

**2c. Analysis of early G2/M arrest in MCF7 cells transfected with small fragment, containing BRCA1-motif 6.** After a detailed analysis of the binding regions between BRCA1 and Filamin A we confirmed that motif 6 of BRCA1 contribute to the binding to Filamin A. However, the main region of BRCA1 that is responsible for the binding to Filamin A is another conserved motif within the BRCA1 N-terminus called motif 2. Please, refer to fig.1 and fig.2 of the paper "Identification of Filamin A as a BRCA1-interacting protein required for efficient DNA repair. 2010, Cell Cycle 2010; 9(7): 1-13, which is attached in the appendices of this report. Moreover, introduction of BRCA1 mutation Y179C in motif 2 disrupts the binding between BRCA1 and Filamin A. Y179C mutation of BRCA1 was found in families with breast and ovarian cancer. Thus, these experiments analyzed the role of Motif 6 and Motif 2 in cell cycle regulation (refer to p.6 of this report where the paper is attached). Thus, this task is completed.

**2d. Performing G2/M checkpoint recovery assays in M2 cell line transfected with pCMV2 Flag-Filamin A construct and simultaneously with pCMV2 Flag-Filamin A and BRCA1 shRNA.**

This task will be performed within next year according to the original plan.

*Thus, Task 2 is going according to plan and should be completed within the next year.*

In conclusion, we are on track to complete the tasks in the time proposed. Our expectations are that within next year we will be able to finish specific aim 2 as it is planned in the application.

### **III. Reportable outcomes**

#### **Publications**

The DOD pre-doctoral fellowship gave me an opportunity to publish a first author paper, which is attached. This paper was also featured in the cover of Cell Cycle journal (attached) and in a News & Views piece (attached). With this paper I fulfilled the minimum requirements for graduation for Cancer Biology PhD program. We are currently working on another manuscript for publication with some of the work that has been described in this report. My fellowship BC083181 was credited in the following paper:

1. **Velkova A**, Carvalho MA, Johnson JO, Tavtigian SV, Monteiro AN. Identification of Filamin A as a BRCA1-interacting protein required for efficient DNA repair. 2010, Cell Cycle 2010; 9(7): 1-13

#### **Meeting/Conference attended**

As part of my training I participated in Gordon Research Conference “Mutagenesis” August 1-6 2010 in Waterville, ME. I presented a poster entitled “Identification of Filamin A as a BRCA1 interacting protein required for efficient DNA repair”.

**Bulleted list of key research and training accomplishments:**

- Verifying the expression level of BRCA1 full-length (WT or mutants) in HCC1937 cell line (task1c)
- Performing colony forming assay after irradiation (task1d)
- Performing early G2/M checkpoint assay (task 1e)
- Performing Radio-Resistant DNA synthesis assay (task 1f)
- Performing spindle assembly checkpoint assay (task 1g)
- Performing dose response and time course analysis in M2, A7, HCT116, HCT116 chk2-/- cell lines (task 2a)
- Publication of paper: Velkova A, Carvalho MA, Johnson JO, Tavtigian SV, Monteiro AN. Identification of Filamin A as a BRCA1-interacting protein required for efficient DNA repair. 2010, Cell Cycle 2010; 9(7):1-13. This paper was also featured on the cover of Cell Cycle journal (attached) and in a *News & Views* piece (attached).
- Presentation of poster: Gordon Research Conference "Mutagenesis" August 1-6, 2010 in Waterville, ME. I presented a poster entitled "Identification of Filamin A as a BRCA1 interacting protein required for efficient DNA repair".

**Conclusion:**

The purpose of this research is to classify *BRCA1* variants for which cancer association is not known (unclassified variants UCV). To approach this problem we hypothesized that poorly characterized but conserved domains in *BRCA1* directly participate in its tumor suppression function. To test this hypothesis we choose a global approach analyzing several *BRCA1* domains and point mutants in functions that have previously been attributed to *BRCA1*: long term survival after irradiation, early G2/M checkpoint, intra-S phase checkpoint, and spindle assembly checkpoint. We successfully optimized conditions for expression of full-length *BRCA1* mutants in two different cell lines by electroporation and lipofectamine based transfection. We analyzed all the *BRCA1* mutants proposed in this application. Our analysis revealed that the coiled-coil domain of *BRCA1* is important for the intra-S-phase checkpoint function of *BRCA1*. We also begin to characterize two conserved motifs of *BRCA1*: Motif 6 (proposed in this application) and Motif 2 (as a new finding). This will have a significant impact not only to understand *BRCA1* role as a tumor suppressor in breast cancer but also to help patients that are carriers of *BRCA1* mutation to make informed clinical decisions.

# Identification of filamin A as a BRCA1-interacting protein required for efficient DNA repair

Aneliya Velkova,<sup>1,2</sup> Marcelo A. Carvalho,<sup>1,†</sup> Joseph O. Johnson,<sup>3</sup> Sean V. Tavtigian<sup>4</sup> and Alvaro N.A. Monteiro<sup>1,\*</sup>

<sup>1</sup>Risk Assessment, Detection and Intervention Program; and <sup>3</sup>Analytic Microscopy Core; H. Lee Moffitt Cancer Center & Research Institute; Tampa, FL USA;

<sup>2</sup>University of South Florida Cancer Biology PhD Program; Tampa, FL USA; <sup>4</sup>Department of Oncological Sciences; Huntsman Cancer Institute; University of Utah, Salt Lake City, UT USA

<sup>†</sup>Current address: Instituto Federal do Rio de Janeiro; Rio de Janeiro, RJ Brazil

**Key words:** BRCA1, filamin A, DNA-PK, non-homologous end joining, DNA damage, DNA repair

**Abbreviations:** ATM, ataxia-telangiectasia mutated; ATR, ATM and Rad3-related; ATRIP, ATR-interacting protein; DDR, DNA damage response; DMEM, dulbecco's modified eagle medium; DNA-PKcs, DNA protein kinase catalytic subunit; DSB, double stranded breaks; FLNA, filamin A; γ-H2AX, histone H2AX phosphorylated at serine 139; GFP, green fluorescent protein; GST, glutathione-sulfo-transferase; GT, glutathione; IR, ionizing radiation; MRN, Mre11/Rad50/NBS1 complex; NHEJ, non-homologous end joining; PI3K, phosphoinositide-3-kinase; RPA, replication protein A; ssDNA, single stranded DNA

The product of the breast and ovarian cancer susceptibility gene BRCA1 has been implicated in several aspects of the DNA damage response but its biochemical function in these processes has remained elusive. In order to probe BRCA1 function we conducted a yeast two-hybrid screening to identify interacting partners to a conserved motif (Motif 6) in the central region of BRCA1. Here we report the identification of the actin-binding protein Filamin A (FLNA) as a BRCA1 partner and demonstrate that FLNA is required for efficient regulation of early stages of DNA repair processes. Cells lacking FLNA display a diminished BRCA1 IR-induced focus formation and a delayed kinetics of Rad51 focus formation. In addition, our data also demonstrate that FLNA is required to stabilize the interaction between components of the DNA-PK holoenzyme, DNA-PKcs and Ku86 in a BRCA1-independent fashion. Our data is consistent with a model in which absence of FLNA compromises homologous recombination and non-homologous end joining. Our findings have implications for the response to radiation-induced DNA damage.

## Introduction

The presence of DNA damage triggers a series of events collectively known as the DNA Damage Response (DDR) pathway.<sup>1,2</sup> Its biological role is to promote efficient DNA repair and to coordinate this activity with cell cycle progression. Injuries to DNA primarily activate three PI3K related kinases ATM, ATR and DNA-PK which are recruited to DNA breaks by the Mre11/Rad50/NBS1 complex, ATRIP and Ku86, respectively.<sup>3</sup> This process is guided by different DNA structures: ATM and DNA-PK are activated by double stranded breaks (DSB) and ATR is activated by Replication Protein A (RPA) coated single stranded DNA (ssDNA).<sup>1</sup>

Two main mechanisms exist to promote DSB repair. The error-prone non-homologous end joining (NHEJ) is functional in all phases of the cell cycle, while the error-free homologous recombination (HR) only functions in S and G<sub>2</sub> phases.<sup>1,2</sup> HR is initiated by ssDNA resulting from resection of DNA ends at the DSB.<sup>1</sup> RPA then binds ssDNA with very high affinity and is visualized as nuclear foci detected by immunofluorescence.<sup>4</sup>

The RPA-coated ssDNA is the substrate for RAD51 recombinase, which is loaded by BRCA2 and mediates the DNA pairing during HR.<sup>1,5</sup> RAD51 co-localizes with the tumor suppressors BRCA1 and BRCA2 in radiation-induced nuclear foci.<sup>6,7</sup> BRCA1 and BRCA2 are part of a complex that controls RAD51 function and the efficiency of HR.<sup>5,8</sup>

Germline mutations in *BRCA1* lead to increased predisposition to breast and ovarian cancer.<sup>9,10</sup> Cloning of *BRCA1* in 1994 made possible the genetic testing of individuals with strong family history of breast cancer and set the stage for an intensive effort to understand its biological functions and the nature of its tumor suppressive activities.<sup>11,12</sup> However, 15 years later it is still not clear which of its many activities can be related directly to its role as tumor suppressor.

*BRCA1* has been implicated in several aspects of the DNA damage response (DDR). Its role in the DDR seems to span a wide range of activities from damage signaling to participation in repair and the coordination of cell cycle checkpoints.<sup>1,13-15</sup> In particular, *BRCA1* has been implicated in HR,<sup>16</sup> microhomology-mediated<sup>17</sup> and NHEJ DNA repair.<sup>18,19</sup>

\*Correspondence to: Alvaro N.A. Monteiro; Email: alvaro.monteiro@moffitt.org

Submitted: 12/10/09; Revised: 01/08/10; Accepted: 01/19/10

Previously published online: www.landesbioscience.com/journals/cc/article/11256

Our laboratory has focused on a systematic analysis of domains and motifs in BRCA1 as a means to understand its biochemical functions.<sup>20</sup> Here we analyzed a conserved region, called Motif 6, spanning amino acids 845–869 coded by BRCA1's large exon 11.<sup>21,22</sup> Using a yeast two hybrid screen we identified the actin-binding protein Filamin A (FLNA) as an interacting partner of BRCA1. Interestingly, FLNA has been shown to interact with BRCA2 and to participate in the DDR.<sup>23–25</sup> Cells lacking FLNA exhibit prolonged checkpoint activation leading to accumulation of cells in G<sub>2</sub>/M after ionizing radiation.<sup>23</sup>

We show that BRCA1 and FLNA interact in mammalian cells and this interaction is mediated by Motif 6 and by another uncharacterized region in BRCA1 N-terminus called Motif 2.<sup>21</sup> Binding to BRCA1 is mediated by the C-terminus of FLNA, a region that includes its dimerization domain. Introduction of a BRCA1 missense variant found in individuals with family history of breast cancer abrogates the interaction. Lack of FLNA leads to a broad defect in DNA repair with accumulation of ssDNA combined with the hyperactivation of ATM and ATR-mediated signaling. We show that this phenotype is due to a combined failure of Ku86 and DNA-PKcs to form stable complexes, and to defects in BRCA1 and Rad51 focus formation implicating FLNA in the control of DNA repair.

## Results

**BRCA1 motif 6 interacts with filamin A.** In order to identify interactors to the conserved Motif 6 of BRCA1 spanning amino acid residues 845–869 (Suppl. Fig. 1A) we performed a yeast two-hybrid screening against a human mammary gland cDNA library. Two overlapping clones coding for human Filamin A (FLNA; OMIM # 300017), spanning amino acid residues 2443–2647 and 2477–2647 (Suppl. Fig. 1B), were identified. This region includes repeat 23, the hinge region, and repeat 24 in the C-terminus FLNA (Suppl. Fig. 1B).<sup>26</sup> We mapped the minimal region of FLNA that interacts with BRCA1 Motif 6 by testing binding of a series of FLNA deletion mutants (Suppl. Fig. 1B). Only the fragment aa 2477–2647 was able to bind BRCA1 Motif 6 (Suppl. Fig. 1B).

Next, we tested whether endogenous FLNA interacted with endogenous BRCA1 in mammalian cells. Immunoprecipitation using a specific monoclonal antibody against BRCA1 pulled down FLNA in HeLa and HCT116 cells (Fig. 1A). In addition, immunoprecipitation using an antibody against FLNA was able to pull down BRCA1 (Fig. 1A). Thus, BRCA1 and FLNA interact in vivo and the interaction is mediated by the C-terminus of FLNA.

Because FLNA and BRCA1 have been demonstrated to be primarily cytoplasmic and nuclear, respectively, we biochemically fractionated HCT116 cells to determine in which subcellular compartment the interaction occurs (Suppl. Fig. 1C). We found that FLNA is expressed in the nucleus and cytoplasm and BRCA1 can be co-immunoprecipitated by FLNA in the nuclear fraction (Suppl. Fig. 1C). We also determined that the interaction is direct as bacterially expressed GST-tagged BRCA1 (aa 141–302) can pull down bacterially expressed His-tagged FLNA C-terminus (Suppl. Fig. 1D).

**BRCA1 binding to FLNA is mediated primarily by BRCA1 motif 2.** In the course of our yeast experiments we noted that the interaction between Motif 6 and FLNA was relatively weak (data not shown). Thus, we hypothesized that other regions in BRCA1 might contribute to binding. We co-expressed in-frame fusions of GST to deletion fragments of BRCA1 and a FLAG-tagged FLNA fragment (aa 2477–2647) in 293FT cells (Fig. 1B) to assess each region's contribution to binding.

We immunoprecipitated FLAG-FLNA using  $\alpha$ -FLAG agarose beads and the eluate with FLAG-peptide was separated by SDS-PAGE. Western blot against FLNA and BRCA1 confirmed that FLAG-FLNA was properly folded and interacted with endogenous BRCA1, respectively (Fig. 1C, left). Western blot against GST revealed interaction of FLNA with different fragments of BRCA1 under low stringency (Fig. 1C, left). Interaction with fragments 1 (aa 1–324), 3 (aa 502–802) and 4 (aa 758–1064) was detected even under high stringency conditions (Fig. 1C, right). Reverse pull-downs of endogenous FLNA using GT-beads confirmed that the interaction is mediated by BRCA1 fragments 1, 3 and 4 (Fig. 1D). In both experiments, BRCA1 fragment 1 showed the strongest interaction (Fig. 1C and D).

Fragment 1 (aa 1–324) includes the RING finger (aa 1–101)<sup>11</sup> and nuclear export signals (aa 22–30 and aa 81–99).<sup>27,28</sup> To determine whether the interaction was mediated by these motifs we used deletion mutants of BRCA1 fragment 1 (Fig. 2A). Initially, we identified BRCA1 residues 141–240 as the interacting region to FLNA (aa 2477–2647) (Fig. 2A). Further mapping identified residues 160–190 as the minimal region required for binding (Fig. 2B). This region, called Motif 2, had been previously identified as conserved motif in *BRCA1* orthologs.<sup>21,22</sup>

To assess whether BRCA1 and FLNA interaction might contribute to breast cancer we searched the Breast Cancer Information Core database (research.ncbi.nih.gov/bic/) for variants in this region. Variant Y179C is a frequent missense change recorded in the database (BIC Database). Introduction of BRCA1 Y179C mutant significantly reduced BRCA1 interaction to FLAG-FLNA aa 2477–2647 and to endogenous FLNA (Fig. 2C) further demonstrating the specificity of the interaction. Because other regions in BRCA1 besides Motif 2 also contributed to the binding we investigated whether the Y179C mutation would disrupt binding to FLNA in the context of full length BRCA1. Introduction of the Y179C mutation significantly reduced the interaction in the full length context as compared to wild type BRCA1 (Fig. 2C, right). In summary, these experiments demonstrate that Motif 2 primarily mediates the interaction to FLNA. Taken together these data raised the possibility that lack of FLNA might impair BRCA1 foci formation after DNA damage. Thus, the following experiments were directed at assessing the role of the interaction in the DNA damage response.

**FLNA-null cells are deficient in DSB repair.** To further characterize the functional significance of FLNA/BRCA1 interaction we obtained the M2 melanoma cell line which lacks FLNA and its counterpart A7 which was obtained by reconstituting M2 cells with full length FLNA cDNA.<sup>29</sup> First, we assessed the kinetics of double strand break (DSB) repair after ionizing radiation (IR). We irradiated or mock treated the FLNA<sup>−</sup> and FLNA<sup>+</sup> cell lines and

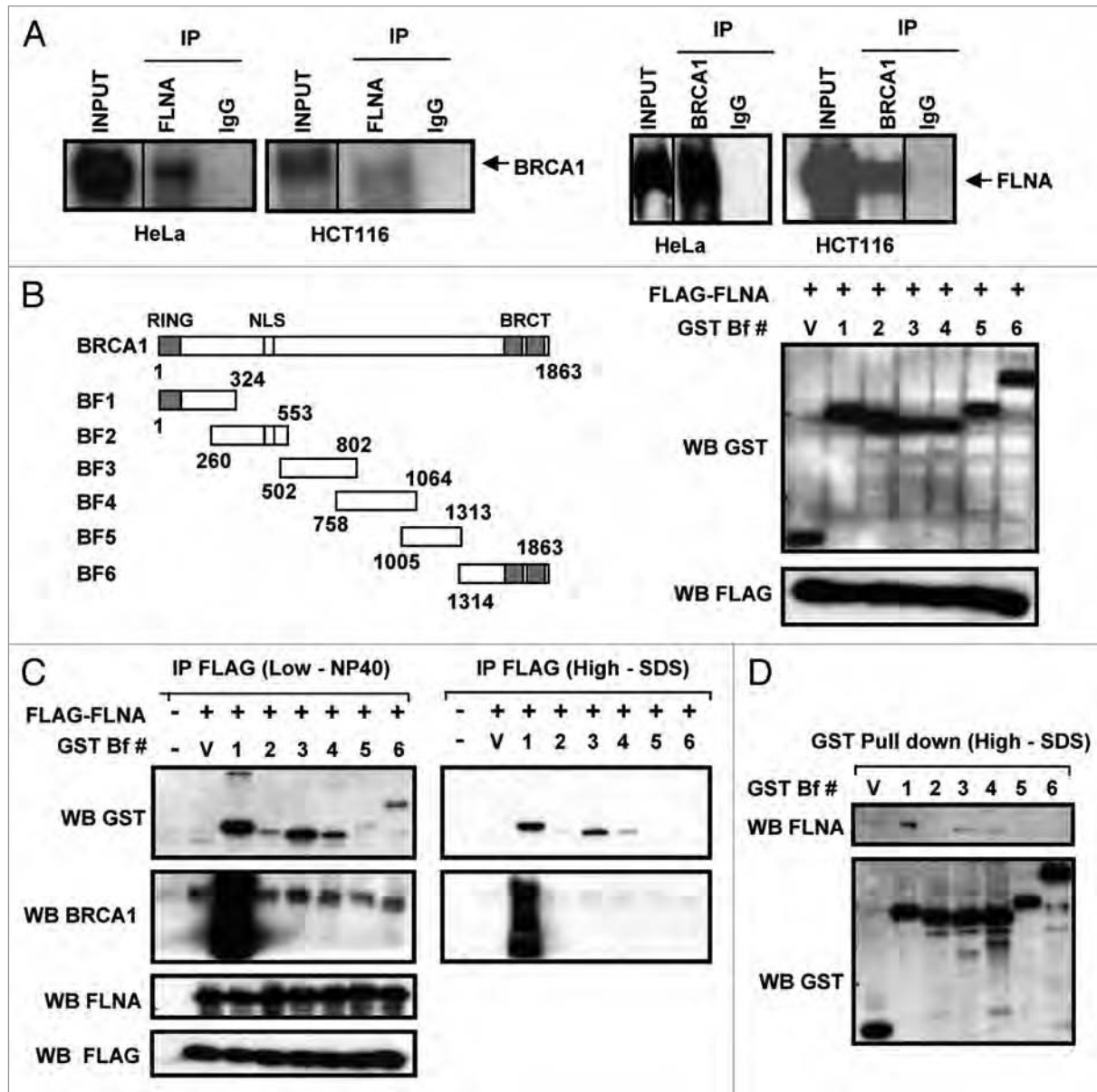


**Figure 1.** Interaction of Filamin A and BRCA1 in mammalian cells. (A) Left, co-immunoprecipitation of endogenous BRCA1 with FLNA in HeLa and HCT116 cells showing interaction of endogenous BRCA1 and FLNA. Right, reverse reaction showing co-immunoprecipitation of endogenous FLNA with BRCA1. Vertical lines indicate where lanes were digitally removed. Figures are not a composite of lanes from two different blots but from the same blot. (B) Left, diagram of deletion constructs used to map the BRCA1 interaction site to FLNA. RING, RING finger domain; NLS, nuclear localization signals; BRCT, BRCA1 C-terminal domains. Right, co-expression of GST-fragments of BRCA1 and FLAG-FLNA (aa 2477–2647) in 293FT cells. Lower molecular weight band obtained in the empty vector (V) transfection corresponds to GST. (C) Co-immunoprecipitation of BRCA1 fragments (WB GST), endogenous BRCA1 (WB BRCA1) with FLAG-FLNA (aa 2477–2647) under low (left panel) and high (right panel) stringency conditions. Note that endogenous FLNA is also immunoprecipitated by FLAG-FLNA (aa 2477–2647) confirming it is in the native conformation (WB FLNA). Strong reactivity shown for GST BF1 is due to recognition of the GST-BRCA1 fragment that contains the epitope for the antibody. (D) GST-pull down experiments show that GST-BRCA1 fragments 1, 3 and 4 can precipitate endogenous FLNA (WB FLNA).

collected cells at several time points after IR. We monitored the presence of DSB with an antibody against histone H2AX phosphorylated at Serine 139 (called  $\gamma$ -H2AX), a marker for DSBs.<sup>30</sup> Whereas the FLNA<sup>+</sup> cell line efficiently repaired DSBs and by 8 h after IR there was no detectable  $\gamma$ -H2AX (Fig. 3A), FLNA<sup>-</sup> cells had a sustained high level of  $\gamma$ -H2AX for up to 32 h after IR. We confirmed this observation using Comet assays (Fig. 3B).

**FLNA deficiency does not cause a defect in sensing DNA damage.** Next, we assessed whether cells lacking FLNA had a compromised DNA damage signaling. Thus, we tested whether ATM and ATR were properly activated upon DNA damage. Phosphorylation of ATM S1981 was not compromised in FLNA<sup>-</sup> cells (Fig. 3C, Top). Likewise, phosphorylation of CHK2 T68 and CHK1 S317, markers of ATM and ATR activation, respectively,

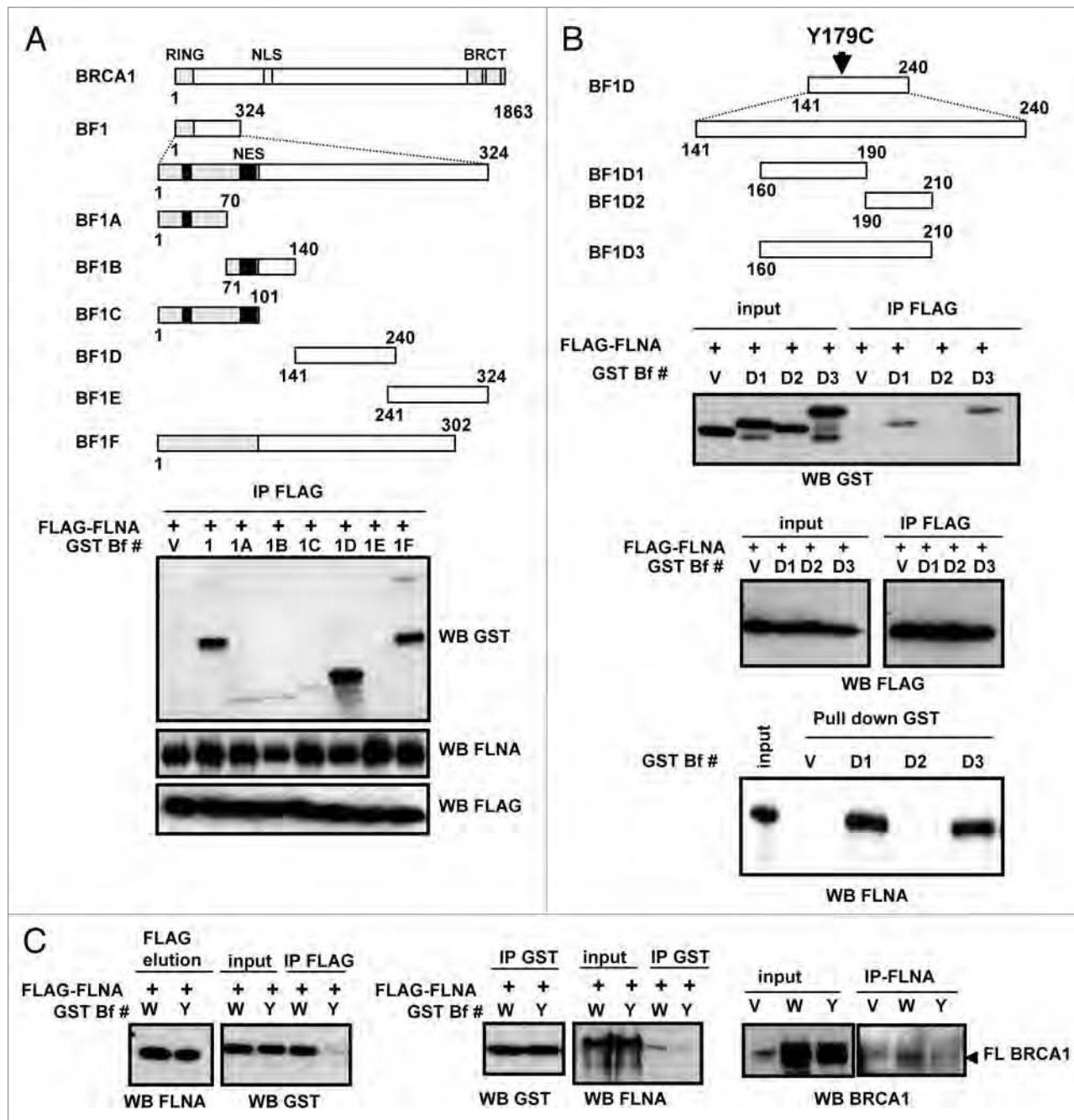


**Figure 2.** Fine mapping of the interaction regions in BRCA1. (A) Upper, diagram of deletion constructs used to map the interaction site to FLNA. NES, nuclear export sequence (black boxes). Lower, FLAG-FLNA (aa 2477–2647) interacts strongly with GST-BRCA1 fragments BF1 (aa 1–324), BF1D (aa 141–240) and BF1F (aa 1–302). (B) First, diagram of deletion constructs of fragment aa 141–240 used to map the interaction site to FLNA. The location of the missense variant Y179C is indicated. Second, FLAG-FLNA (aa 2477–2647) co-immunoprecipitates with GST-BRCA1 fragments BF1D1 (aa 160–190) and BF1D3 (aa 160–210). V, GST; D1, GST-BRCA1 fragment BF1D1 (aa 160–190); D2, GST-BRCA1 fragment BF1D2 (aa 190–210); D3, GST-BRCA1 fragments BF1D3 (aa 160–210). Third, control for expression levels. Fourth, GST-BRCA1 fragments BF1D1 (aa 160–190) and BF1D3 (aa 160–210) can pull down endogenous FLNA. (C) Introduction of BRCA1 Y179C mutation significantly reduces BRCA1 interaction to FLAG-FLNA aa 2477–2647 (Left) and to endogenous FLNA (Middle). W, wild type GST-BRCA1 fragment BF1D (aa 141–240); Y, GST-BRCA1 fragment BF1D with Y179C mutation. Right, Introduction of BRCA1 Y179C mutation into a full length BRCA1 context significantly reduces interaction to endogenous FLNA. W, wild type full length BRCA1; Y, full length BRCA1 carrying a Y179C mutation.

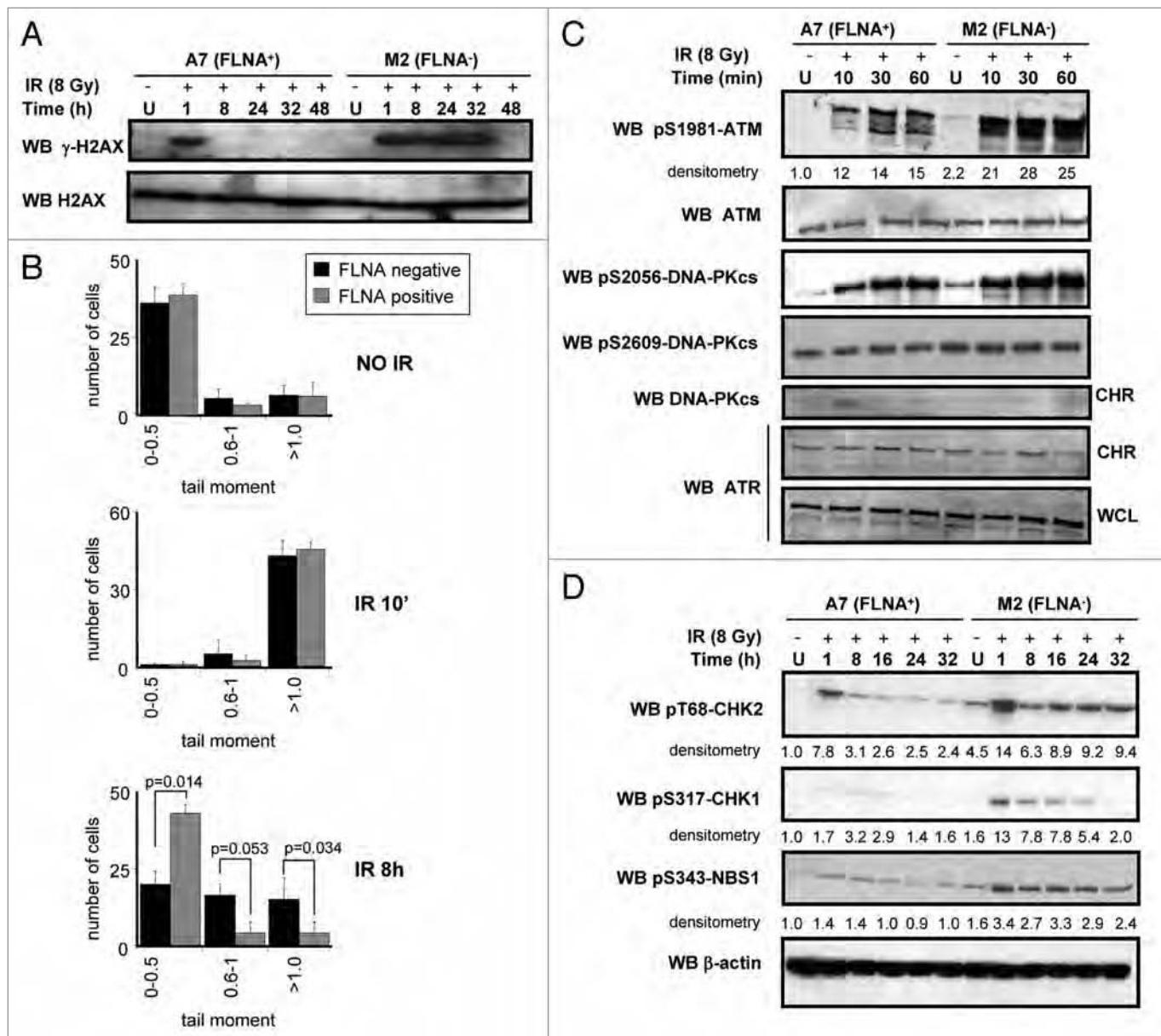


**Figure 3.** FLNA-null cells are deficient in repair but show no impairment in activating the DNA damage response. (A) FLNA<sup>+</sup> (A7) and FLNA<sup>-</sup> (M2) cells were irradiated with 8 Gy or mock-treated (U) and harvested at the indicated time points. While FLNA<sup>+</sup> cells repair most of the DSBs (as measured by  $\gamma$ -H2AX) by 8 h, FLNA<sup>-</sup> cells show significant unrepaired DSBs even after 32 h post-IR (Top). Bottom, shows total levels of H2AX as a loading control. (B) FLNA<sup>+</sup> (A7) and FLNA<sup>-</sup> (M2) cells were irradiated with 8 Gy or mock-treated (NO IR) and harvested at the indicated time points and comet assays were performed under neutral conditions. A two-tailed Student's t test was performed and p values are shown for statistically significant differences. (C) Top two, ATM activation as measured by phosphorylation of S1981 is not compromised in FLNA<sup>-</sup> cells. Blot for total ATM is used as a loading control. Note significantly higher levels of pS1981-ATM in FLNA<sup>-</sup> cells. Middle three, no significant difference was observed in levels of DNA-PKcs S2056 or S2609 phosphorylation but recruitment of DNA-PKcs to chromatin is defective in FLNA<sup>-</sup> cells. Bottom two, ATR presence in chromatin (CHR) is shown. Blot for ATR levels in whole cell lysates is used as a loading control. (D) CHK2, CHK1 and NBS1 activation as measured by pT68-CHK2, pS317-CHK1 and pS343-NBS1, respectively is not compromised in FLNA<sup>-</sup> cells. Note consistently higher levels of pT68-CHK2, pS317-CHK1 and pS343-NBS1 in FLNA<sup>-</sup> cells.  $\beta$ -actin is used as a loading control.

did not show a defect (Fig. 3D). Intriguingly, we consistently observed higher levels of phosphorylation of ATM, CHK2 and CHK1 in cells lacking FLNA (Fig. 3C and D) indicating an upregulation of ATM and ATR signaling. These results confirmed previous data by Meng et al.<sup>23</sup> showing a sustained activation of CHK2 and CHK1 in FLNA-deficient cells following damage.

**FLNA deficiency impairs BRCA1 and Rad51 foci formation.** To determine whether the deficiency in repair was due to defective recruitment of factors required for the DDR we performed immunofluorescence analysis in non-irradiated or irradiated cells at 1 and 24 h after IR. Accumulation of  $\gamma$ -H2AX and pS343-NBS1, early markers of DNA damage, was comparable

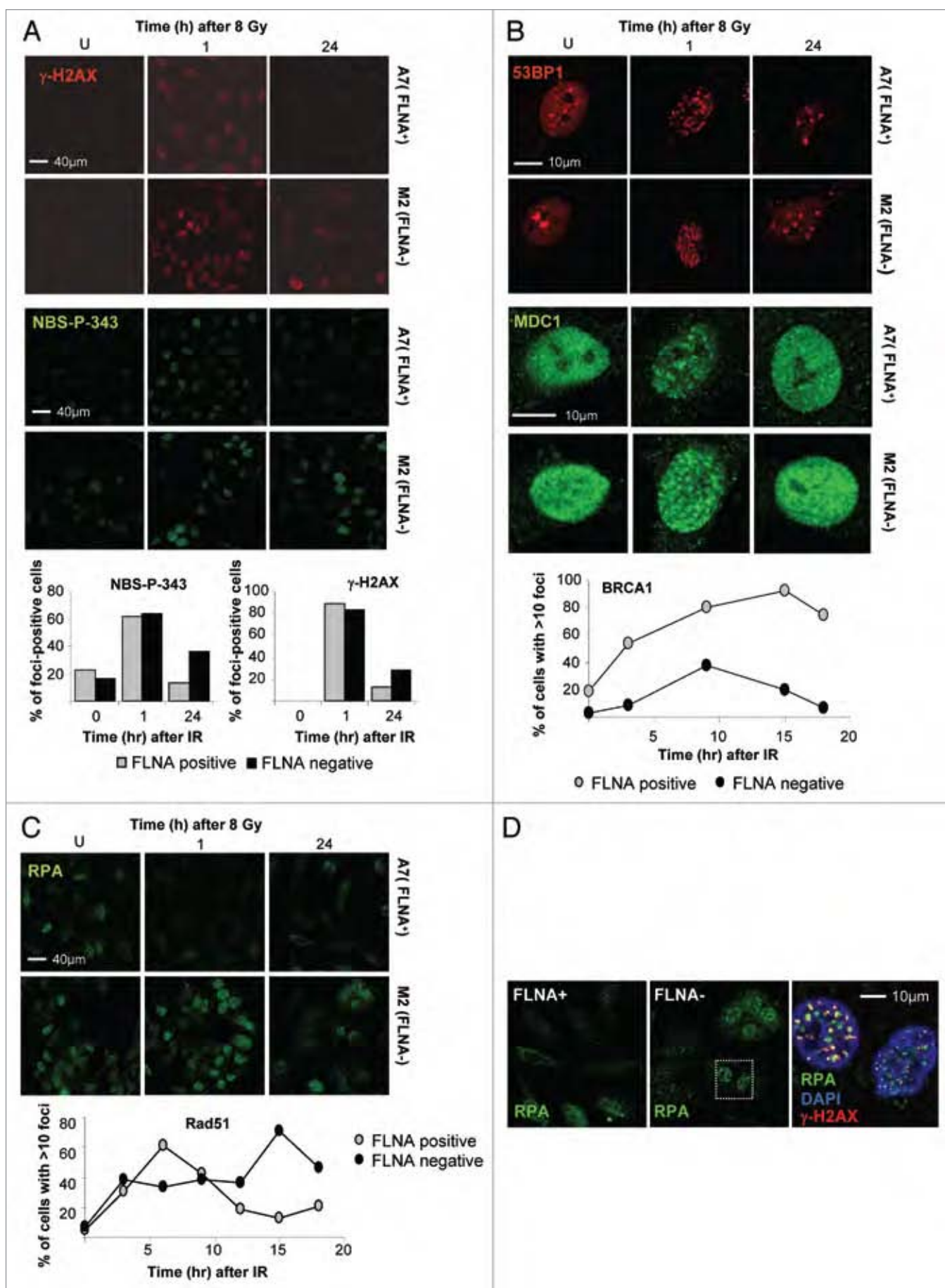


**Figure 4 (See opposite page).** Recruitment of DNA damage response factors to IR-induced foci. (A) Early markers of DNA damage  $\gamma$ -H2AX (red) and phosphoserine 343 NBS1 (green) form foci irrespective of FLNA status. Note maintenance of foci after 24 h only in FLNA<sup>+</sup> cells. Lower, show quantification of foci-positive cells ( $\geq 20$  foci). (B) Recruitment of DNA damage response mediator proteins 53BP1 (red, top) and MDC1 (green, middle) was also comparable at early time points. BRCA1 foci formation was compromised in FLNA-deficient cells (lower). (C) Recruitment of repair factor p34 RPA (green, top) did not show any difference between the cell lines at the early time points. FLNA-deficient cells displayed a delayed kinetics of Rad51 foci formation (bottom). In (A–C) representative results from two independent experiments are shown. In each experiment one slide was scored per time point with at least 50 (A) or 100 (B and C) cells scored per slide. Mock-treated cells are indicated by (U). (D) FLNA-deficient cells present with large chromatin-bound RPA foci at 24 h after IR. Higher magnification of FLNA<sup>+</sup> and FLNA<sup>-</sup> cells after 24 h post-IR. Left, shows FLNA<sup>+</sup> cells stained for RPA (green). Middle, shows FLNA<sup>-</sup> cells stained for RPA (green). Note that nuclear foci are significantly larger than in FLNA<sup>+</sup> cells. Right, shows a blow up of the inset (white square in middle) with staining for DAPI (blue), RPA (green) and  $\gamma$ -H2AX (red).

in both cell lines at 1 h (Fig. 4A). In order to determine if there were small differences we quantified foci-positive cells (Fig. 4A, lower). Results were comparable in both cell lines at 0 and 1 hr after IR, but FLNA-negative cells showed increased number of foci-positive cells after 24 hr. Likewise, recruitment of mediator proteins MDC1, 53BP1, was also comparable at 1 h (Fig. 4B). Finally, repair factor RPA did not show any difference between the cell lines at 1 h (Fig. 4C). Consistent with our western blot results (Fig. 3) where we detected abnormally high levels of  $\gamma$ -H2AX, pT68-CHK2 and pS317-CHK1 at 24 h, we detected persistent foci of  $\gamma$ -H2AX, pS343-NBS1 and RPA at 24 h after irradiation only in FLNA-deficient cells (Fig. 4A–C). Thus, the repair defect in FLNA-deficient cells was not due to a failure to initiate the DNA damage response.

Next, we investigated the ability of BRCA1 and Rad51 to form IR-induced foci. A detailed analysis showed that FLNA-deficient cells are unable to efficiently form BRCA1 IR-induced foci as compared to FLNA-proficient cells (Fig. 4B and bottom). Although Rad51 displayed a comparable initial response at 3 h after IR, it failed to mount a response comparable to FLNA-proficient cells at 6 h after IR. Rad51 presented a delayed kinetics of foci formation with a peak at 15 h in FLNA-deficient cells (Fig. 4C and bottom). Taken together these data suggest that the compromised repair capacity in FLNA-deficient cells may be, at least partially, mechanistically tied to inefficient HR.

**Lack of FLNA leads to accumulation of ssDNA after DNA damage.** During our analysis we noted that RPA foci in FLNA-deficient cells were not only persistent 24 h after damage but were also significantly larger (Fig. 4D). To determine whether those foci were associated with chromatin we pre-extracted cells with Triton X100 before fixation. This method has been successfully used to detect only the fraction of RPA tightly bound to chromatin.<sup>31</sup> Interestingly, FLNA-deficient cells accumulate large chromatin-bound RPA foci whereas FLNA<sup>+</sup> cells present fewer and smaller chromatin-bound RPA foci at 24 h after IR (Fig. 4D). Whereas most FLNA<sup>+</sup> cells have recovered from G<sub>2</sub>/M arrest and represent an asynchronous population at 24 h, most FLNA<sup>-</sup> cells remain arrested in G<sub>2</sub>/M at 24 h after IR.<sup>23</sup> Thus, these large tracts of ssDNA found in FLNA<sup>-</sup> cells are unlikely to be due to replication foci.

**Expression of BRCA1-interacting fragment of FLNA or FLNA-interaction fragment of BRCA1 phenocopies loss of FLNA.** To gain more insight of the mechanism by which FLNA participates in DNA repair we transfected FLNA<sup>+</sup> and FLNA<sup>-</sup> cell lines with flag-tagged Filamin A aa 2477–2647 construct (BRCA1-interacting fragment). For the sake of simplicity we will

refer to this FLNA BRCA1-interacting fragment as FLNA-Bf. At 24 h post transfection we irradiated cells with 8 Gy IR and collected samples at different time points. Transfection of FLNA-Bf did not lead to checkpoint recovery in FLNA<sup>-</sup> cells as measured by phosphorylation of CDC2 Y15 (Fig. 5A). Interestingly, transfection of the same fragment in FLNA<sup>+</sup> cells led to a similar phenotype as that found for FLNA<sup>-</sup> cells as shown by phosphorylation of CDC2 Y15 and H2AX S139 (Fig. 5B). We also confirmed that expression of FLNA-Bf acts in a dominant negative fashion in a stable transfection context (Fig. 5C). We generated HCT116 cells stably expressing GFP-FLNA-Bf or GFP alone that were mock-treated and irradiated. Cells expressing GFP-FLNA-Bf retained high levels of phosphorylated H2AX up to 32 h after damage while cells expressing GFP alone showed levels returning to unirradiated levels at 8 h after damage (Fig. 5C).

Next we asked whether expression of a GST-tagged BRCA1 FLNA-interacting fragment (BRCA1-Ff) could also lead to a dominant negative phenotype (Fig. 5D). In order to verify the specificity of the interaction we transfected a mutated BRCA1-Ff carrying the Y179C mutation and determined whether it lead to a dominant negative phenotype. Introduction of the Y179C mutation (Fig. 2C) significantly reduced the BRCA1-FLNA interaction. The wild type BRCA1-FLNA-Ff led to increased and sustained phosphorylation of CDC2 Y15 and H2AX (Fig. 5D) while the BRCA1-Ff Y179C (Fig. 5D) displayed a dominant negative effect that is intermediate between vector control (Fig. 5B) and the wild type construct (BRCA1-Ff; Fig. 5D). This intermediate effect could be due to the residual binding of BRCA1-Y179C mutant to FLNA. Alternatively, this could also be due to the inability of the mutant to disrupt the binding of FLNA to other regions of endogenous BRCA1 that participate in the interaction (Fig. 1C and D).

**FLNA is required for efficient interactions between DNA-PKcs and Ku86.** Our previous experiments demonstrated that FLNA<sup>-</sup> cells displayed defective DNA repair, showed signs of compromised HR, and accumulated large tracts of ssDNA. Because mammalian cells also repair DSBs using non homologous end joining (NHEJ) we hypothesized that lack of FLNA also had an impact on the NHEJ pathway.

First, we tested whether FLAG-FLNA aa 2477–2647 interacted with NHEJ factors. FLAG-FLNA aa 2477–2647 immunoprecipitated DNA-PKcs in 293FT cells independent of DNA damage (Fig. 6A). To determine whether FLNA was required for the stability of the Ku86/DNA-PKcs complex we performed immunoprecipitation experiments in FLNA<sup>+</sup> and FLNA<sup>-</sup> cell lines in the presence or absence of irradiation (Fig. 6B). Interestingly,

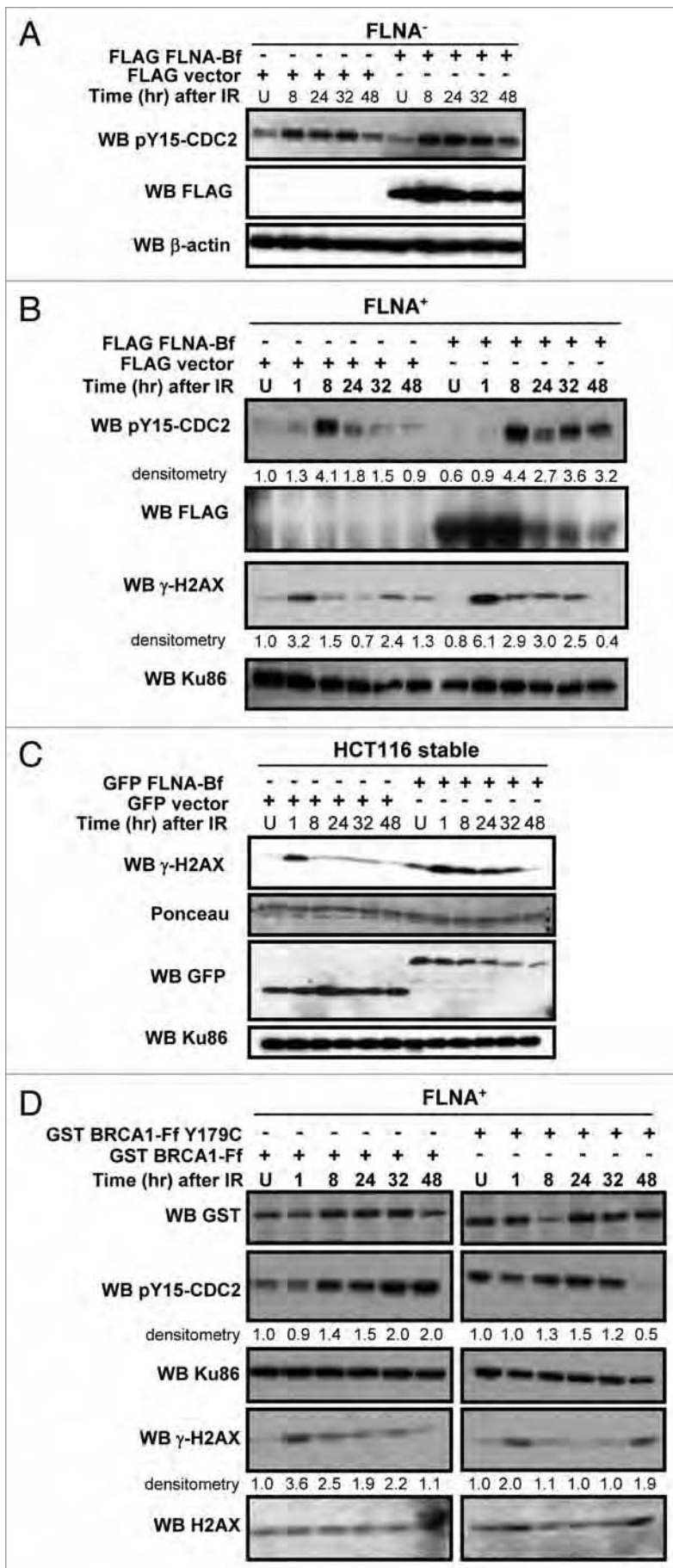


**Figure 5.** Expression of BRCA1-interacting fragment of FLNA or FLNA-interaction fragment of BRCA1 phenocopies loss of FLNA. (A) FLNA<sup>-</sup> cells were transfected with an empty FLAG vector or a FLAG FLNA-Bf constructs. Cells were mock-treated (U) or treated with 8 Gy IR and cells were collected at different time points. Expression of FLAG FLNA-Bf was unable to reverse the recovery defect. (B) FLNA<sup>+</sup> cells were transfected with empty FLAG vector or a FLAG FLNA-Bf constructs. Cells were mock-treated (U) or treated with 8 Gy IR and cells were collected at different time points. Cells expressing of FLAG FLNA-Bf displayed a phenotype similar to FLNA<sup>-</sup> cells. (C) HCT116 cells stably expressing FLAG FLNA-Bf displayed a phenotype similar to FLNA<sup>-</sup> cells. (D) FLNA<sup>+</sup> cells were transfected with a GST BRCA1-Ff or a GST BRCA1-Ff Y179C. Cells were mock-treated (U) or treated with 8 Gy IR and cells were collected at different time points. Only cells expressing of GST BRCA1-Ff but not GST BRCA1-Ff Y179C displayed a phenotype similar to FLNA<sup>-</sup> cells, confirming that the effect is specific.

in FLNA<sup>-</sup> cells Ku86 and DNA-PKcs complex formation was compromised in IR-treated and untreated cells (Fig. 6B).

Next we tested whether FLNA was required for Ku86 loading onto chromatin after DNA damage. Ku86 was efficiently recruited to chromatin upon DNA damage in the presence and absence of FLNA (Fig. 6C) while we detected DNA-PKcs in chromatin only in the presence of FLNA (Fig. 3B). Interestingly, loading of Ku86 onto chromatin persisted longer and with consistently higher levels in FLNA<sup>-</sup> than in FLNA<sup>+</sup> cells (Fig. 6C).

Finally, we tested whether BRCA1 was required to stabilize the interaction between DNA-PKcs and Ku86. We examined *BRCA1*-deficient HCC1937 cell line<sup>32</sup> and a HCC1937 derivative reconstituted with full length BRCA1 (gift from Junjie Chen). Complex formation between Ku86 and DNA-PKcs was not dependent on BRCA1 under IR-treated or untreated conditions (Suppl. Fig. 2B).

In summary, our results indicate that cells lacking FLNA have a defect in the two principal mechanisms for double strand break repair. Mechanistically, FLNA impacts on HR by contributing to efficient recruitment of BRCA1 and Rad51 to IR-induced foci, and on NHEJ by promoting the stability of the DNA-PKcs and Ku86 complex.

## Discussion

In this paper we shed light on the mechanism by which Filamin A (FLNA) is required for efficient DNA repair. Our data indicates that lack of FLNA impacts on HR and NHEJ. FLNA is an actin-binding protein and its inactivation leads to an array of disorders such as otopalatodigital spectrum disorder, Melnick-Needles syndrome and periventricular heterotopia.<sup>26</sup> Although of unclear significance, at least two families carrying germline mutations in *BRCA1*

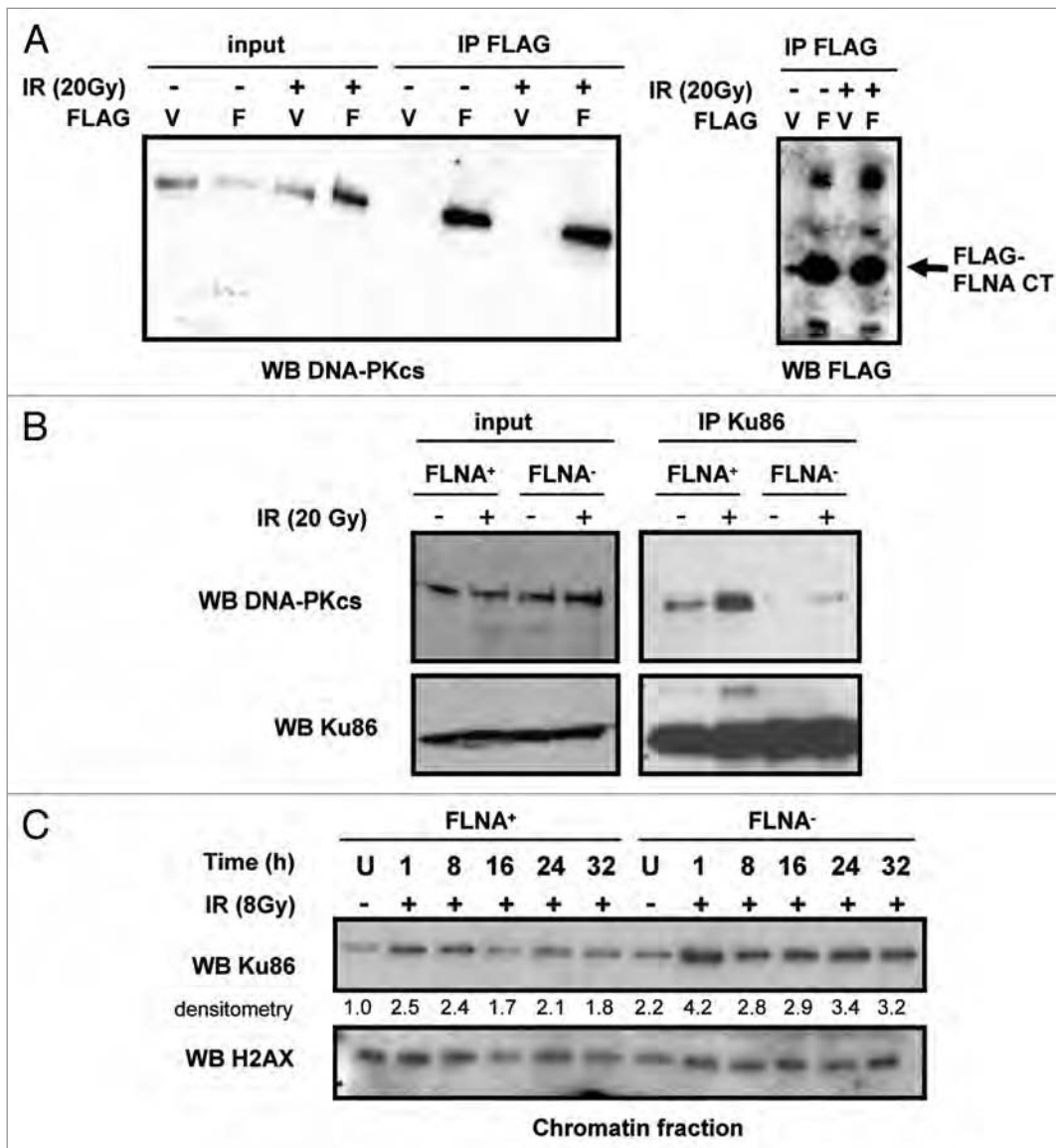


**Figure 6.** FLNA interacts in vivo with DNA-PKcs and mediates its interaction to Ku86. (A) Left, 293FT cells were transfected with FLAG-FLNA aa 2477–2647 (F) or empty FLAG vector (V) and mock-treated or irradiated with 20 Gy. Cells were collected after 1 h and immunoprecipitated using  $\alpha$ -FLAG antibody. FLAG-FLNA aa 2477–2647 co-immunoprecipitates DNA-PKcs in the presence and absence of IR. Right, control for expression and the efficiency of the immunoprecipitation. (B) The interaction between DNA-PKcs and Ku86 is compromised in cells lacking FLNA. Left, shows that levels of DNA-PKcs and Ku86 are similar in both cell lines and in the presence and absence of irradiation. Right, shows that Ku86 and DNA-PKcs interact in FLNA<sup>+</sup> cells in the absence of damage and complex formation is significantly increased in the presence of irradiation. Complex formation in the presence and absence of IR is severely compromised in FLNA<sup>-</sup> cells. (C) Loading of Ku86 onto chromatin after DNA damage is increased in FLNA<sup>+</sup> cells. Histone H2AX levels are used as a loading control.

have been shown to manifest ventricular heterotopia.<sup>33,34</sup> FLNA interacts with a variety of proteins, including BRCA2,<sup>25</sup> and deficiency in FLNA leads to sensitivity to DNA damage and a defect in the recovery from G<sub>2</sub> arrest.<sup>23</sup> Thus, we investigated further its role in the DNA damage response.

FLNA binds BRCA1 using its extreme C-terminus which contains its dimerization domain. BRCA1 interaction with FLNA is mediated by a 30 amino acid region in the N-terminus of BRCA1 which contains a conserved domain called Motif 2.<sup>21</sup> Introduction of the Y179C mutation in Motif 2 significantly decreases the interaction. Analyses by the Align GV-GD method

or by a yeast-based recombination assay suggest that Y179C may act as a deleterious mutation.<sup>35,36</sup> On the other hand, this variant has been found co-occurring in trans with a known deleterious mutation, which indicates that it is unlikely to have severe effects.<sup>37</sup> Thus, the Y179C may constitute a hypomorphic mutation with moderate effects on breast cancer predisposition. Of note, Motif 2 is close to the region that has been implicated in binding of BRCA1 to Ku86.<sup>38</sup>

In order to dissect the molecular role of FLNA in the DDR we took advantage of a well-characterized genetically-defined system. A melanoma cell line lacking FLNA was isolated and subsequently

reconstituted with FLNA yielding a pair of cell lines in which the only difference is the presence or absence of FLNA.<sup>29</sup> When we irradiated FLNA<sup>-</sup> and FLNA<sup>+</sup> cells, we noticed that FLNA<sup>-</sup> took much longer to resolve DSBs (Fig. 3A and B). To elucidate the mechanism underlying the repair defect we systematically investigated the proficiency of damage signaling in FLNA<sup>-</sup> cells.

Initially we investigated the recruitment and activation kinetics of the upstream kinases, as well as their downstream substrates after DNA damage. We found that FLNA deficiency led to the hyperactivation of ATM as judged by phosphorylation of ATM S1981 and CHK2 T68, surrogate markers of ATM activation.<sup>39-41</sup> Similarly, lack of FLNA also led to a hyperactivation of ATR, as measured by CHK1 S317 phosphorylation, a marker for ATR activation.<sup>42</sup> Moreover, we also found sustained levels of phosphorylation of NBS1 S343 to be higher in FLNA<sup>-</sup> cells. Although the role of NBS1 phosphorylation in the DNA damage signaling is poorly understood, it is generally thought to reflect ATM and ATR activation.<sup>43,44</sup> We also determined that major mediator proteins BRCA1, MDC1 and 53BP1 formed IR-induced foci irrespective of FLNA status. However, BRCA1 foci formation was significantly impaired in FLNA-deficient cells. In addition, Rad51 foci formation displayed a delayed kinetics in cells lacking FLNA. These data indicate that FLNA-deficient cells have impaired homologous recombination. Indeed, during the preparation of this manuscript Yue et al. showed that FLNA-deficient cells have a reduced ability to repair I-SceI-induced DSBs.<sup>45</sup>

During the course of our experiments we noticed a consistent increase in the number of FLNA<sup>-</sup> cells displaying IR-induced RPA foci. These foci progressively increased in size at later time points after IR. RPA is a ssDNA binding protein and participates in DNA metabolism processes where there is generation of ssDNA such as replication, repair and recombination.<sup>46,47</sup> Phosphorylation leads to inability of RPA to associate with the replication centers and leads to the association with DNA damage-induced foci instead.<sup>48</sup> Interestingly, lack of NHEJ proteins DNA-PKcs and Ku86, which together with Ku70 form the active DNA-PK complex, leads to accumulation of ssDNA in S phase.<sup>49</sup> Thus, we further investigated how the lack of FLNA impacted on DNA-PK complex formation.

Remarkably, Ku86 failed to interact with DNA-PKcs in the absence of FLNA. The reduced stability of the interaction is not due to Ku86 failure to load onto chromatin, as FLNA<sup>-</sup> cells displayed sustained higher levels of chromatin-bound Ku86 than FLNA<sup>+</sup> cells after damage. Ku86 is one of the first molecules to bind DNA ends after DSBs<sup>50</sup> and recruits DNA-PKcs via its C-terminus.<sup>3</sup> Taken together these results establish that lack of FLNA results in an unstable association of Ku86 and DNA-PKcs impairing the function of the complex. This impaired DNA-PK activity leads to a continuous build up of ssDNA and Ku86 on chromatin.

Over 16 phosphorylation sites have been identified in DNA-PKcs although their role is still poorly understood. Nevertheless, DNA-PKcs phosphorylation status is thought to influence its activity.<sup>51</sup> DNA-PKcs interacts with Ku86 and free ends of DNA in an unphosphorylated form,<sup>52</sup> and autophosphorylation is required for NHEJ progression.<sup>53</sup> Thus, we investigated the

status of the two major phosphorylation clusters in DNA-PKcs, namely the 2056 and 2609 clusters. Clusters 2056 and 2609 were consistently phosphorylated upon treatment with IR irrespective of FLNA status. The fact that DNA-PKcs is phosphorylated upon damage in the absence of FLNA suggests that DNA-PKcs is interacting with the Ku86/DNA complex albeit transiently. Alternatively, it is possible that phosphorylation of DNA-PKcs is not mediated by autophosphorylation at the synaptic complex but rather via hyperactive ATM and ATR in FLNA-deficient cells.

We showed that FLNA and BRCA1 interact and that FLNA deficiency leads to a marked decrease in BRCA1 foci formation after damage. To investigate further the role of BRCA1 we tested whether expression of the BRCA1 FLNA-interacting fragment in FLNA-proficient cells could also act in a dominant negative fashion leading to a phenotype similar to FLNA-deficient cells. Strikingly, expression of the BRCA1-Ff lead to a defect in DNA repair as judged by CDC2 pY15 and  $\gamma$ -H2AX markers. This effect is specific because expression of BRCA1-Ff containing a mutation that disrupts FLNA/BRCA1 interaction does not lead to the same phenotype. Taken together, these data establish that BRCA1 participates in the FLNA-dependent regulation of the DNA damage response.

Our data shows that absence of FLNA leads to defective DSB repair. The defect is a combined result of compromised HR and NHEJ processes. At this stage we cannot distinguish whether FLNA-deficiency leads to a defective step that is common to both pathways or, alternatively, it impacts different steps in these pathways. In fact, the interplay between these two arms of the DNA repair process is not fully understood,<sup>54</sup> in particular after IR, which generates an array of different DNA modifications. The observed phenotype is consistent with a model in which Ku86 recognizes and binds free ends of DNA, but in the absence of FLNA, fails to make a stable complex with DNA-PKcs. We propose that unstable Ku86/DNA-PKcs interaction results in impaired end processing, accumulation of ssDNA, and hyperactivation of DNA damage signaling.

In addition, in FLNA-deficient cells BRCA1 displays impaired foci formation suggesting that FLNA also plays a role in stabilizing BRCA1 at the DSBs. BRCA1 colocalizes with Rad50/Mre11/NBS1 complex at IR-induced foci<sup>55,56</sup> and inhibits Mre11 exonuclease activity.<sup>57</sup> Thus, the diminished amounts of BRCA1 at IR-foci may lead to an unregulated Mre11 exonuclease activity with formation of the observed extended tracts of RPA-coated ssDNA in FLNA-deficient cells (Fig. 4C and D). BRCA1 has also been implicated in the regulation of Rad51,<sup>7,58</sup> although the mechanism by which it happens is obscure.<sup>59</sup> The kinetics of Rad51 foci formation in FLNA-deficient cells suggests that there is no problem in the initial recruitment to foci (see Fig. 4C, bottom, 3 h time point). The extended plateau observed in Rad51 foci (from 3 to 12 h after IR) may indicate an accumulation of DSBs that do not fulfill the end processing requirements for efficient Rad51 loading. Although further research will be needed to test this proposed model, it provides a tractable system to dissect the interplay between different processes involved in DNA repair.

It is possible that FLNA provides a framework for the assembly of factors in the synaptic complex. While unrepai

yeast (which lacks recognizable DNA-PKcs and FLNA orthologs) migrates to so-called DNA repair centers,<sup>60</sup> the picture is different in mammalian cells where broken chromosome ends are essentially immobile.<sup>61,62</sup> It will be interesting to determine whether lack of FLNA affects the mobility of broken ends.

## Materials and Methods

**Constructs.** GST-fusion fragments of BRCA1 in the mammalian expression vector pEBG BF 1-6 were a gift from Toru Ouchi. BRCA1 fragments BF1A (aa 1-70), BF1B (aa 71-140), BF1C (aa 1-101), BF1D (aa 141-240), BF1D1 (aa 160-190), BF1D2 (aa 190-210), BF1D3 (aa 160-210), BF1E (aa 241-324) and BF1F (aa 1-302) were obtained by PCR using pEBG BF1 as template (primer sequences are available upon request). The PCR products were digested and cloned into pEBG vector<sup>63</sup> and sequenced. Construct BF1D Y179C was obtained by site directed mutagenesis using BF1D as template for the PCR reaction. FLAG FLNA-Bf was obtained by cloning a PCR fragment of FLNA (aa 2477-2647) in frame to FLAG in pCMV2-FLAG vector.

**Cell lines and transfections.** The FLNA-deficient M2 melanoma cell line and its isogenic cell line, A7, reconstituted with full length FLNA cDNA<sup>29</sup> (gift from Thomas Stossel) was grown in MEM (Sigma) with 8% newborn calf serum (Sigma) and 2% fetal bovine serum (FBS; SAFC Biosciences, Lenexa, KS). A7 cells were grown in the presence of 0.2 mg/ml G418 (Fisher). HeLa (ATCC, Manassas, VA) was grown in DMEM with 5% FBS (Sigma). HCT116 (ATCC) was grown in McCoy's with 10% FBS. 293FT (InVitrogen) cells were grown in DMEM media (Sigma) with 10% FBS. Tissue culture media was supplemented with penicillin and streptomycin. Transfections were performed using Fugene 6 (Roche) according to the manufacturer's instructions.

**Antibodies.** The following antibodies, peptides and beads were used:  $\alpha$ -BRCA1 mouse monoclonal antibody MS110 (Ab-1; Calbiochem; San Diego, CA) and SG11 (gift from Livingston D);  $\alpha$ -Filamin A mouse monoclonal antibody PM6/317 (Chemicon International);  $\alpha$ -FLAG M2 mouse monoclonal antibody (Sigma); 3xFLAG-peptide (Sigma);  $\alpha$ -GST goat polyclonal antibody (Pharmacia Biotech); GT-sepharose 4B beads (GE Healthcare);  $\alpha$ -Ku86 monoclonal antibody B-1 and  $\alpha$ -Rad51 rabbit polyclonal antibody H-92 (Santa Cruz Biotechnology, Inc., Santa Cruz, CA);  $\alpha$ -TP53BP1 mouse monoclonal antibody and  $\alpha$ -phosphoserine 343-NBS1 mouse monoclonal antibody (Upstate Biotechnology);  $\alpha$ -p34 RPA mouse monoclonal antibody Ab-1 and  $\alpha$ -DNA-PKcs mouse monoclonal antibodies Ab-2 (Neomarkers, Freemont, CA);  $\alpha$ -phosphoserine 2056 DNA-PKcs rabbit polyclonal antibody (Abcam, Cambridge, MA);  $\alpha$ -phosphoserine 2609 DNA-PKcs rabbit polyclonal antibody (Novus Biologicals);  $\alpha$ -MDC1 (SIGMA);  $\gamma$ -H2AX rabbit polyclonal;  $\alpha$ -H2AX;  $\alpha$ -phosphoserine 1981 ATM;  $\alpha$ -ATM;  $\alpha$ -ATR;  $\alpha$ -phosphothreonine 68 CHK2;  $\alpha$ -phosphoserine 317 CHK1 (Cell Signaling);  $\alpha$ - $\beta$  actin (Sigma). Conjugates for immunofluorescence were Alexa fluor 488 or 555 Molecular Probes.

**Immunoprecipitation, pull-downs, western blot analysis and densitometry.** Whole cell extracts were prepared by lysing cells

in a mild RIPA buffer (120 mM NaCl, 50 mM Tris pH 7.4, 1% NP40, 1 mM EDTA, protease inhibitors, 4 mM PMSF) lacking harsher SDS, sodium deoxycholate, and Triton X-100 detergents. The same buffer was used for immunoprecipitation. For high stringency immunoprecipitations the RIPA buffer was supplemented with 0.5% SDS. Antibodies (1  $\mu$ g) were pre-incubated with protein A/G agarose beads (Santa Cruz Biotechnology, Inc.,), washed twice in RIPA buffer and incubated with the cell extracts overnight at 4°C. After incubation, the slurry were pelleted by centrifugation (2,000 rpm) and washed twice by removing the supernatant. Sample buffer was added to the beads and boiled for 10 min. For GST-pull downs, cell extracts were incubated with GT-beads, washed in RIPA buffer, and boiled.

Samples for western blot analysis were separated by SDS-PAGE and gels were electroblotted on a wet apparatus to a PVDF membrane. The PVDF membrane was blocked with 5% milk in TBS buffer containing 0.1% Tween (TBS-Tween) for 1 h. The membrane was washed three times in TBS-Tween and the antibody was added in 0.5% milk in TBS-Tween. The membrane was washed three times in TBS-Tween and incubated with the appropriate conjugate. After final washes Blots were incubated with ECL (Millipore, Billerica, MA).

Chromatin fractions were obtained by lysing the cells with mild RIPA buffer and centrifuging at 14,000 rpm for 5 min. The pellet was then washed twice in mild RIPA and extracted with acid extraction buffer (0.5 M HCl, 10% Glycerol, 100 mM BME) and subsequently neutralized using 40 mM Tris pH 7.4 with protease inhibitors and NaOH.

Western blot data was quantified by densitometry using AlphaEaseFC v 3.1.2. Each lane was normalized using the corresponding loading controls and then expressed as a fold change relative to the untreated FLNA<sup>+</sup> cells in each blot.

**Immunofluorescence.** For BRCA1 analysis cells were fixed with 4% formaldehyde for 5 min followed by 5 min incubation with 100% ethanol. Cells were permeabilized with 0.25% Triton X-100 in PBS for 10 min, washed with PBS, and then blocked for 30 min with 5% BSA in PBS at room temperature (RT). After blocking, BRCA1 monoclonal antibody (SG11; kind gift from David Livingston) was added to 1% BSA in PBS for 1 h RT. Cells were washed and goat  $\alpha$ -mouse Alexa Fluor 488 (Molecular Probes) was added for an additional 1 h RT.

For all other antibodies, cells were plated onto chamber slides and after 24 h they were washed with cytoskeleton buffer (10 mM HEPES/KOH pH 7.4, 300 mM sucrose, 100 mM NaCl, 3 mM MgCl<sub>2</sub>) and fixed with 4% formaldehyde for 30 min RT. For analysis of chromatin bound RPA cells were pre-extracted for 2 min on ice with cytoskeleton buffersupplemented with 0.5% Triton X-100 before fixation.<sup>64</sup> After fixation cells were permeabilized with 0.25% Triton X-100 in PBS for 5 min RT and then washed and blocked with 5% BSA in PBS for 30 min RT. Primary and secondary antibodies in 1% BSA in PBS were added for 1 h each.

Cells were washed and mounted with Prolong Gold medium (Molecular Probes). Images were taken on a Leica Confocal Microscope. For quantification of BRCA1 and Rad51 immunofluorescence foci approximately 100 cells were scored per each

time point. Cells were scored as foci-positive if they presented with more than 10 foci per cell (an example can be found in Supp. Fig. 2A). For  $\gamma$ -H2AX and NBS-P-343 at least 50 cells per time point were counted for each condition. Cells were scored as foci-positive if they presented with more than 20 foci per cell. A threshold of 20 foci was chosen based on the number of foci found in unirradiated samples using the described antibodies. Determination of foci number per cell was done using Definiens Developer XD 1.1 (Definiens AD, Germany). A rule set was developed to segment nuclei based on the DAPI stain and then segment foci within the nucleus based on an intensity threshold. Representative results from at least two independent experiments are shown instead of statistical data on a small number of measurements with variability as recently recommended.<sup>65</sup>

**Comet assay.** Comet assays were performed in neutral conditions using a comet assay kit (Trevigen, Gaithersburg, MD) according to manufacturer's instructions. Briefly, cells were collected at the indicated time points, combined in low melting agarose (Trevigen, Gaithersburg, MD), spread over the comet slide area and allowed to set. Then, slides were immersed in lysis buffer for 30 min at 4°C. Electrophoresis was run in TBE buffer for 20 min at 1 V/cm voltage. Image analysis was done with Comet Analysis System 2.3.3 software (Loats Associates Inc., Westminster, MD).

## References

- Jackson SP, Bartek J. The DNA-damage response in human biology and disease. *Nature* 2009; 461:1071-8.
- Harper JW, Elledge SJ. The DNA damage response: ten years after. *Mol Cell* 2007; 28:739-45.
- Falck J, Coates J, Jackson SP. Conserved modes of recruitment of ATM, ATR and DNA-PKcs to sites of DNA damage. *Nature* 2005; 434:605-11.
- Raderschall E, Golub EI, Haaf T. Nuclear foci of mammalian recombination proteins are located at single-stranded DNA regions formed after DNA damage. *Proc Natl Acad Sci USA* 1999; 96:1921-6.
- San Filippo J, Sung P, Klein H. Mechanism of eukaryotic homologous recombination. *Annu Rev Biochem* 2008; 77:229-57.
- Scully R, Chen J, Plug A, Xiao Y, Weaver D, Feunteun J, et al. Association of BRCA1 with Rad51 in mitotic and meiotic cells. *Cell* 1997; 88:265-75.
- Chen J, Silver DP, Walpita D, Cantor SB, Gazdar AF, Tomlinson G, et al. Stable interaction between the products of the BRCA1 and BRCA2 tumor suppressor genes in mitotic and meiotic cells. *Mol Cell* 1998; 2:317-28.
- Greenberg RA, Sobhian B, Pathania S, Cantor SB, Nakatani Y, Livingston DM. Multifactorial contributions to an acute DNA damage response by BRCA1/BARD1-containing complexes. *Genes Dev* 2006; 20:34-46.
- Ford D, Easton DF, Bishop DT, Narod SA, Goldgar DE. Risks of cancer in BRCA1-mutation carriers. *Breast Cancer Linkage Consortium. Lancet* 1994; 343:692-5.
- Easton DF, Bishop DT, Ford D, Crockford GP. Genetic linkage analysis in familial breast and ovarian cancer: results from 214 families. *The Breast Cancer Linkage Consortium. Am J Hum Genet* 1993; 52:678-701.
- Miki Y, Swensen J, Shattuck-Eidens D, Futreal PA, Harshman K, Tavtigian S, et al. A strong candidate for the breast and ovarian cancer susceptibility gene BRCA1. *Science* 1994; 266:66-71.
- Friedman LS, Ostermeyer EA, Szabo CI, Dowd P, Lynch ED, Rowell SE, et al. Confirmation of BRCA1 by analysis of germline mutations linked to breast and ovarian cancer in ten families. *Nat Genet* 1994; 8:399-404.
- Narod SA, Foulkes WD. BRCA1 and BRCA2: 1994 and beyond. *Nat Rev Cancer* 2004; 4:665-76.
- Scully R, Livingston D. In search of the tumour-suppressor functions of BRCA1 and BRCA2. *Nature* 2000; 408:429-32.
- Venkitaraman AR. Cancer Susceptibility and the Functions of BRCA1 and BRCA2. *Cell* 2002; 108:171-82.
- Moynahan ME, Chiu JW, Koller BH, Jasin M. Brca1 controls homology-directed DNA repair. *Mol Cell* 1999; 4:511-8.
- Zhong Q, Chen CF, Chen PL, Lee WH. BRCA1 facilitates microhomology-mediated end joining of DNA double strand breaks. *J Biol Chem* 2002; 277:28641-7.
- Zhuang J, Zhang J, Willers H, Wang H, Chung JH, van Gent DC, et al. Checkpoint kinase 2-mediated phosphorylation of BRCA1 regulates the fidelity of nonhomologous end-joining. *Cancer Res* 2006; 66:1401-8.
- Wang HC, Chou WC, Shieh SY, Shen CY. Ataxia telangiectasia mutated and checkpoint kinase 2 regulate BRCA1 to promote the fidelity of DNA end-joining. *Cancer Res* 2006; 66:1391-400.
- Carvalho MA, Marsillac SM, Karchin R, Manoukian S, Grist S, Swaby RF, et al. Determination of Cancer Risk Associated with Germ Line BRCA1 Missense Variants by Functional Analysis. *Cancer Res* 2007; 67:1494-501.
- Orelli BJ, Logsdon JM Jr, Bishop DK. Nine novel conserved motifs in BRCA1 identified by the chicken orthologue. *Oncogene* 2001; 20:4433-8.
- Abkevich V, Zharkikh A, Deffenbaugh AM, Frank D, Chen Y, Shattuck D, et al. Analysis of missense variation in human BRCA1 in the context of interspecific sequence variation. *J Med Genet* 2004; 41:492-507.
- Meng X, Yuan Y, Maestas A, Shen Z. Recovery from DNA damage-induced G<sub>2</sub> arrest requires actin-binding protein filamin-A/actin-binding protein 280. *J Biol Chem* 2004; 279:6098-105.
- Yue J, Wang Q, Lu H, Brenneman M, Fan F, Shen Z. The cytoskeleton protein filamin-A is required for an efficient recombinational DNA double strand break repair. *Cancer Res* 2009; 69:7978-85.
- Yuan Y, Shen Z. Interaction with BRCA2 suggests a role for filamin-1 (hsFLNa) in DNA damage response. *J Biol Chem* 2001; 276:48318-24.
- Feng Y, Walsh CA. The many faces of filamin: a versatile molecular scaffold for cell motility and signalling. *Nat Cell Biol* 2004; 6:1034-8.
- Rodriguez JA, Henderson BR. Identification of a functional nuclear export sequence in BRCA1. *J Biol Chem* 2000; 275:38589-96.
- Thompson ME, Robinson-Benion CL, Holt JT. An amino-terminal motif functions as a second nuclear export sequence in BRCA1. *J Biol Chem* 2005; 280:21854-7.
- Cunningham CC, Gorlin JB, Kwiatkowski DJ, Hartwig JH, Janmey PA, Byers HR, et al. Actin-binding protein requirement for cortical stability and efficient locomotion. *Science* 1992; 255:325-7.
- Rogakou EP, Boon C, Redon C, Bonner WM. Megabase chromatin domains involved in DNA double-strand breaks in vivo. *J Cell Biol* 1999; 146:905-16.
- Dimitrova DS, Gilbert DM. Stability and nuclear distribution of mammalian replication protein A heterotrimeric complex. *Exp Cell Res* 2000; 254:321-7.
- Tomlinson GE, Chen TT, Stastny VA, Virmani AK, Spillman MA, Tonk V, et al. Characterization of a breast cancer cell line derived from a germ-line BRCA1 mutation carrier. *Cancer Res* 1998; 58:3237-42.
- Eccles DM, Barker S, Pilz DT, Kennedy C. Neuronal migration defect in a BRCA1 gene carrier: possible focal nullisomy? *J Med Genet* 2003; 40:24.
- Eccles D, Bunyan D, Barker S, Castle B. BRCA1 mutation and neuronal migration defect: implications for chemoprevention. *J Med Genet* 2005; 42:42.
- Tavtigian SV, Deffenbaugh AM, Yin L, Judkins T, Scholl T, Samollow PB, et al. Comprehensive statistical study of 452 BRCA1 missense substitutions with classification of eight recurrent substitutions as neutral. *J Med Genet* 2006; 43:295-305.
- Caligo MA, Bonatti F, Guidugli L, Aretini P, Galli A. A yeast recombination assay to characterize human BRCA1 missense variants of unknown pathological significance. *Hum Mutat* 2009; 30:123-33.

## Acknowledgements

The authors are indebted to members of the Monteiro Lab for helpful discussions and to Marcus Smolka and Ed Seto for a critical reading of the manuscript, to David Livingston and Arcangela De Nicolo for a generous gift of SG-11 antibody; Thomas Stossel for the M2 and A7 cell lines; Junjie Chen for the HCC1937-BRCA1wt cells; and Toru Ouchi for GST-BRCA1 constructs. This paper is dedicated to the memory of Hidesaburo Hanafusa, Professor Emeritus of the Rockefeller University, who passed away on March 15, 2009.

## Financial disclosure

This work was supported by a predoctoral fellowship [BC083181] to A.V. from the US Department of Defense Breast Cancer Research Program; a National Institutes of Health grant [CA116167]; a grant from the Florida Breast Cancer Coalition Foundation to A.M.; and supported in part by the Analytic Microscopy and the Molecular Biology cores at the H.L. Moffitt Cancer Center & Research Institute.

## Note

Supplementary materials can be found at:  
[www.landesbioscience.com/supplement/VelkovaCC9-7-Sup.pdf](http://www.landesbioscience.com/supplement/VelkovaCC9-7-Sup.pdf)

37. Judkins T, Hendrickson BC, Deffenbaugh AM, Eliason K, Leclair B, Norton MJ, et al. Application of embryonic lethal or other obvious phenotypes to characterize the clinical significance of genetic variants found in trans with known deleterious mutations. *Cancer Res* 2005; 65:10096-103.

38. Wei L, Lan L, Hong Z, Yasui A, Ishioka C, Chiba N. Rapid recruitment of BRCA1 to DNA double-strand breaks is dependent on its association with Ku80. *Mol Cell Biol* 2008; 28:7380-93.

39. Bakkenist CJ, Kastan MB. DNA damage activates ATM through intermolecular autophosphorylation and dimer dissociation. *Nature* 2003; 421:499-506.

40. Matsuoka S, Rotman G, Ogawa A, Shiloh Y, Tamai K, Elledge SJ. Ataxia telangiectasia-mutated phosphorylates Chk2 in vivo and in vitro. *Proc Natl Acad Sci USA* 2000; 97:10389-94.

41. Melchionna R, Chen XB, Blasina A, McGowan CH. Threonine 68 is required for radiation-induced phosphorylation and activation of Cds1. *Nat Cell Biol* 2000; 2:762-5.

42. Cimprich KA, Cortez D. ATR: an essential regulator of genome integrity. *Nat Rev Mol Cell Biol* 2008; 9:616-27.

43. Gatei M, Young D, Cerosaletti KM, Desai-Mehta A, Spring K, Kozlov S, et al. ATM-dependent phosphorylation of nibrin in response to radiation exposure. *Nat Genet* 2000; 25:115-9.

44. D'Amours D, Jackson SP. The Mre11 complex: at the crossroads of dna repair and checkpoint signalling. *Nat Rev Mol Cell Biol* 2002; 3:317-27.

45. Yue J, Wang Q, Lu H, Brenneman M, Fan F, Shen Z. The cytoskeleton protein filamin-A is required for an efficient recombinational DNA double strand break repair. *Cancer Res* 2009; 69:7978-85.

46. Ifrode C, Daniely Y, Borowiec JA. Replication protein A (RPA): the eukaryotic SSB. *Crit Rev Biochem Mol Biol* 1999; 34:141-80.

47. Golub EI, Gupta RC, Haaf T, Wold MS, Radding CM. Interaction of human rad51 recombination protein with single-stranded DNA binding protein, RPA. *Nucleic Acids Res* 1998; 26:5388-93.

48. Vassil VM, Wold MS, Borowiec JA. Replication protein A (RPA) phosphorylation prevents RPA association with replication centers. *Mol Cell Biol* 2004; 24:1930-43.

49. Karlsson KH, Stenerlow B. Extensive ssDNA end formation at DNA double-strand breaks in non-homologous end-joining deficient cells during the S phase. *BMC Mol Biol* 2007; 8:97.

50. Mahaney BL, Meek K, Lees-Miller SP. Repair of ionizing radiation-induced DNA double-strand breaks by non-homologous end-joining. *Biochem J* 2009; 417:639-50.

51. Weterings E, Chen DJ. DNA-dependent protein kinase in nonhomologous end joining: a lock with multiple keys? *J Cell Biol* 2007; 179:183-6.

52. Calsou P, Frit P, Humbert O, Muller C, Chen DJ, Salles B. The DNA-dependent protein kinase catalytic activity regulates DNA end processing by means of Ku entry into DNA. *J Biol Chem* 1999; 274:7848-56.

53. Reddy YV, Ding Q, Lees-Miller SP, Meek K, Ramsden DA. Non-homologous end joining requires that the DNA-PK complex undergo an autophosphorylation-dependent rearrangement at DNA ends. *J Biol Chem* 2004; 279:39408-13.

54. Yun MH, Hioni K. CtIP-BRCA1 modulates the choice of DNA double-strand-break repair pathway throughout the cell cycle. *Nature* 2009; 459:460-3.

55. Wu X, Petrini JH, Heine WF, Weaver DT, Livingston DM, Chen J. Independence of R/M/N focus formation and the presence of intact BRCA1. *Science* 2000; 289:11.

56. Zhong Q, Chen CF, Li S, Chen Y, Wang CC, Xiao J, et al. Association of BRCA1 with the hRad50-hMre11-p95 complex and the DNA damage response. *Science* 1999; 285:747-50.

57. Paull TT, Cortez D, Bowers B, Elledge SJ, Gellert M. Direct DNA binding by Brca1. *Proc Natl Acad Sci USA* 2001; 98:6086-91.

58. Chen JJ, Silver D, Cantor S, Livingston DM, Scully R. BRCA1, BRCA2 and Rad51 operate in a common DNA damage response pathway. *Cancer Res* 1999; 59:1752-6.

59. Cousineau I, Abaji C, Belmaaza A. BRCA1 regulates RAD51 function in response to DNA damage and suppresses spontaneous sister chromatid replication slippage: implications for sister chromatid cohesion, genome stability and carcinogenesis. *Cancer Res* 2005; 65:11384-91.

60. Lisby M, Mortensen UH, Rothstein R. Colocalization of multiple DNA double-strand breaks at a single Rad52 repair centre. *Nat Cell Biol* 2003; 5:572-7.

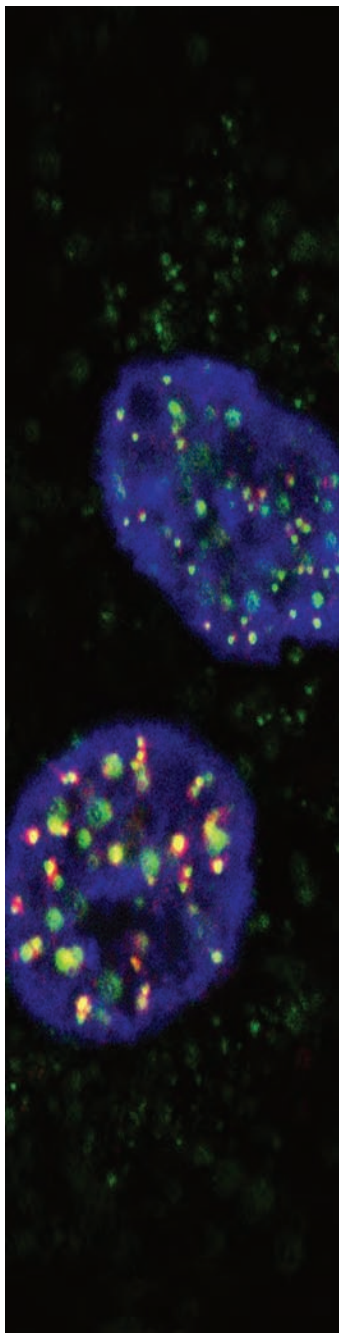
61. Misteli T, Soutoglou E. The emerging role of nuclear architecture in DNA repair and genome maintenance. *Nat Rev Mol Cell Biol* 2009; 10:243-54.

62. Soutoglou E, Dorn JF, Sengupta K, Jasin M, Nussenzweig A, Ried T, et al. Positional stability of single double-strand breaks in mammalian cells. *Nat Cell Biol* 2007; 9:675-82.

63. Tanaka M, Gupta R, Mayer BJ. Differential inhibition of signaling pathways by dominant-negative SH2/SH3 adapter proteins. *Mol Cell Biol* 1995; 15:6829-37.

64. Dimitrova DS, Todorov IT, Melendy T, Gilbert DM. Mcm2, but not RPA, is a component of the mammalian early G<sub>1</sub>-phase prereplication complex. *J Cell Biol* 1999; 146:709-22.

65. Editorial. How robust is your data? *Nat Cell Biol* 2009; 11:667-70.

**Editorial Board**

Frederick W. Alt  
*Children's Hospital*  
Jiri Bartek  
*Institute of Cancer Biology*  
John Blenis  
*Harvard Medical School*  
Judith Campisi  
*Lawrence Berkeley National Lab.*  
Lewis Cantley  
*Harvard Institutes of Medicine*  
Xuetao Cao  
*National Key Laboratory*  
Duncan J. Clarke  
*University of Minnesota*  
Carlo M. Croce  
*Kimmel Cancer Center*  
Zbigniew Darzynkiewicz  
*New York Medical College*  
Ronald A. DePinho  
*Harvard University*  
Julian Downward  
*Cancer Research UK*  
Brian J. Druker  
*Oregon Health Science University*  
Wafik S. El-Deriy  
*University of Pennsylvania*  
Stephen J. Elledge  
*Harvard Medical School*  
Gerard Evan  
*University of California, San Francisco*  
David E. Fisher  
*Harvard University*  
Tito Fojo  
*National Institutes of Health*  
Stephen H. Friend  
*Merck*  
Paraskevi Giannakakou  
*Weill Medical College of Cornell University*  
Steven Grant  
*Medical College of Virginia*  
Douglas Green  
*St. Jude Children's Hospital*  
Andrei V. Gudkov  
*Roswell Park Cancer Institute*  
Michael N. Hall  
*University of Basel*

Philip W. Hinds  
*Tufts Medical Center*  
Tim Hunt  
*Cancer Research UK*  
Tony Hunter  
*The Salk Institute*  
Matt Kaeberlein  
*University of Washington*  
Brian K. Kennedy  
*University of Washington*  
Daniel J. Kliensky  
*University of Michigan*  
Eugene V. Koonin  
*National Institutes of Health*  
Guido Kroemer  
*INSERM*  
David P. Lane  
*Institute of Molecular and Cell Biology*  
Arnold Levine  
*Institute for Advanced Study*  
Beth Levine  
*UT Southwestern Medical Center*  
Chiang J. Li  
*ArQuile Biomedical Institute*  
Michael P. Lisanti  
*Kimmel Cancer Center*  
James A. McCubrey  
*East Carolina University*  
Gerry Melino  
*University of Rome*  
Donald Metcalf  
*The Royal Melbourne Hospital*  
Yusuke Nakamura  
*University of Tokyo*  
Paul Nurse  
*Rockefeller University*  
Andre Nussenzweig  
*National Institutes of Health*  
Moshe Oren  
*The Weizmann Institute of Science*  
Arthur B. Pardee  
*Harvard University*  
Helen Piwnica-Worms  
*Washington University*  
George C. Prendergast  
*Thomas Jefferson University*

Carol Prives  
*Columbia University*  
Martin Raff  
*University College London*  
E. Premkumar Reddy  
*Temple University*  
John C. Reed  
*The Burnham Institute for Medical Research*  
Steven I. Reed  
*The Scripps Research Institute*  
James M. Roberts  
*Fred Hutchinson Cancer Research Center*  
Igor B. Roninson  
*Ordway Research Institute*  
Martine Roussel  
*St. Jude's Children's Hospital*  
Leo Sachs  
*The Weizmann Institute of Science*  
Paolo Sassone-Corsi  
*University of California, Irvine*  
Charles L. Sawyers  
*Memorial Sloan-Kettering Cancer Center*  
Charles J. Sherr  
*St. Jude's Children's Hospital*  
Frank Slack  
*Yale University*  
Gary S. Stein  
*University of Massachusetts*  
Qing-Yuan Sun  
*Chinese Academy of Sciences*  
George F. Vande-Woude  
*Van Andel Research Institute*  
Bert Vogelstein  
*Johns Hopkins University*  
Peter K. Vogt  
*The Scripps Research Institute*  
Karen Vousden  
*Beatson Institute for Cancer Research*  
Paul Workman  
*Cancer Research UK*  
Michael B. Yaffe  
*Massachusetts Institute of Technology*  
Yi-Xin Zeng  
*Sun Yat-sen University*  
Harald zur Hausen  
*Deutsches Krebsforschungszentrum*

docks to the centromere is still unknown.<sup>10</sup> The data presented here suggest that the tertiary DNA structure is important for CPC docking to the centromere and it would be interesting to appreciate if DNA structure contributes directly to recruitment of the CPC to the inner centromere or if CPC docking is mediated through other chromatin binding proteins.

In summary, this work provides strong indications that the CPC can directly regulate the mitotic checkpoint and can prevent anaphase

onset independently of its microtubule destabilizing activity. However, the mechanism by which the CPC is involved in signaling to the mitotic checkpoint remains unclear and future work that addresses these issues will be required.

#### Acknowledgements

We thank Dr. Gerben Vader for useful comments and The Netherlands Organization for Scientific Research (Vidi 917.66.332) for support.

#### References

1. Musacchio A, et al. *Nat Rev Mol Cell Biol* 2007; 8:379-93.
2. Ruchaud S, et al. *Nat Rev Mol Cell Biol* 2007; 8:798-812.
3. Pinsky BA, et al. *Nat Cell Biol* 2006; 8:78-83.
4. Kallio MJ, et al. *FASEB J* 2001; 15:2721-3.
5. Hauf S, et al. *J Cell Biol* 2003; 161:281-94.
6. Vader G, et al. *Mol Biol Cell* 2007; 18:4553-64.
7. Ditchfield C, et al. *J Cell Biol* 2003; 161:267-80.
8. Liu D, et al. *Science* 2009; 323:1350-3.
9. Emanuele MJ, et al. *J Cell Biol* 2008; 181:241-54.
10. Vader G, et al. *J Cell Biol* 2006; 173:833-7.

## Filamins and the potential of complexity

Comment on: Velkova A, et al. *Cell Cycle* 2010; 9:1421-33.

Thomas P. Stossel; Harvard Medical School; Boston, MA USA; Email: Tstossel@partners.org

"Filamin," the name given by Wang and Singer to a high molecular-weight protein they identified in chicken gizzard smooth muscle, has become generic for a family of proteins, the first example of which was purified from rabbit lung macrophages. Humans express three filamin genes, filamin A, the first identified and most abundant filamin of nonmuscle tissues, filamin B, also widely expressed in nonmuscle cells and now known to be the variant named by Wang and Singer, and filamin C, mainly found in muscle cells.<sup>1</sup>

Initial research on filamins focused on their actin filament crosslinking properties and established that they very efficiently create elastic actin gels by promoting orthogonal branching of cross-linked actin filaments.<sup>2</sup> Structural analysis of filamin molecules has revealed how as extended dimers with multiple actin-binding domains they accomplish such branching.<sup>3</sup> Increasingly sophisticated studies on the elasticity of filamin-actin networks have implicated filamins, particularly filamin A, as mediators of the mechanical resistance of many living cells.<sup>4</sup>

In recent years identification of an astonishingly large number of filamin A binding partners, including diverse membrane proteins, signaling intermediates and transcription factors has dominated filamin research (Figure 1).<sup>5</sup> Since homozygous filamin A deficiency is embryonic lethal,<sup>6</sup> a growing list of degenerative diseases associated with filamin mutations probably reflects functional disruption

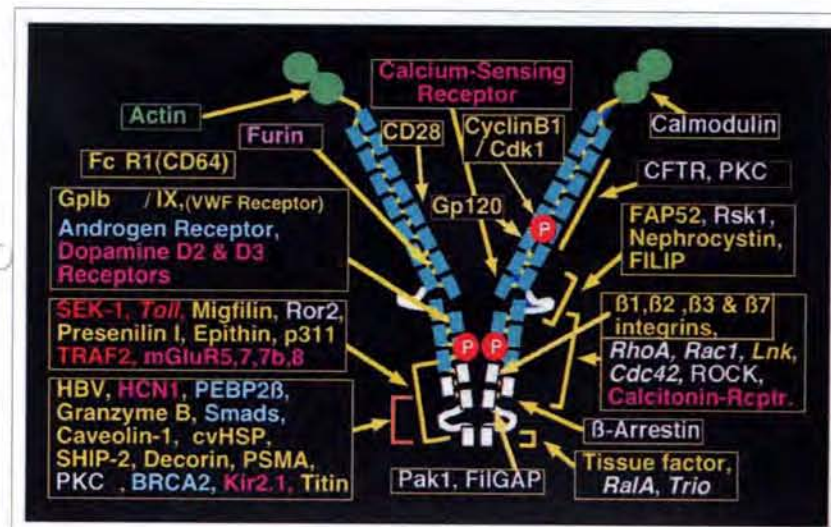


Figure 1. Filamin A binding partners and their location on its subunits.

of filamin-partner interactions.<sup>7-9</sup> The paper by Velkova et al. in the previous issue of *Cell Cycle* describing a role for filamin A in DNA repair function of BRCA-1 adds cancer to the disease list. Since the filamin-partner binding must in many cases be cell-specific and temporally limited, for example, during embryonic development, targeting the binding interfaces might provide relatively specific and minimally toxic therapies for diseases. If posterity can rise to this challenge, it would exemplify how complexity, while daunting, can be useful.

#### References

1. Stossel T, et al. *Nat Rev Cell Mol Biol* 2001; 2:138-45.
2. Hartwig JH, et al. *J Mol Biol* 1981; 145:563-81.
3. Nakamura F, et al. *J Cell Biol* 2007; 179:1011-25.
4. Koenderink G, et al. *Proc Natl Acad Sci USA* 2009; 106:15192-7.
5. Zhou A-X, et al. *Trends Cell Biol* 2010; 20:113-22.
6. Feng Y, et al. *Proc Natl Acad Sci USA* 2006; 103:19836-41.
7. Robertson S, et al. *Am J Med Genet A* 2006; 140A:1726-36.
8. Kyndt F, et al. *Circulation* 2007; 115:40-9.
9. Schröder R, et al. *Brain Pathol* 2009; 19:483-92.